[American Journal of Science, Vol. 315, September, 2015, P. 589–619, DOI 10.2475/07.2015.01]

American Journal of Science

SEPTEMBER 2015

MULTIPLE MANTLE SOURCES OF THE EARLY PERMIAN PANJAL TRAPS, KASHMIR, INDIA

J. GREGORY SHELLNUTT*,†, GHULAM M. BHAT**, KUO-LUNG WANG***, MENG-WAN YEH*, MICHAEL E. BROOKFIELD§, and BOR-MING JAHN§§

ABSTRACT. The Early Permian Panjal Traps of northern India are the volcanic remnants of continental rifting that led to the formation of the Neotethys Ocean and the ribbon-like continent Cimmeria. The Traps are one of at least five major mafic eruptions of flood basalts during the Late Palaeozoic however their origin and petrogenesis are poorly constrained. Basalts from the Kashmir Valley were collected and analyzed for chemical and isotopic (Sr, Nd) compositions in order to characterize their mantle source and evaluate the petrogenetic processes related to opening of the Neotethys Ocean. Samples collected from the eastern side (Guryal Ravine, Pahalgam, PJ3) of the Kashmir Valley are chemically similar to mildly alkaline to tholeiitic, within-plate flood basalts. The TiO_2 contents (TiO_2 = 0.8 to 3.1 wt.%), La/Yb_N values (La/Yb_N = 1.8 to 6.1) and $\varepsilon_{Nd}(t)$ values ($\varepsilon_{Nd}(t) = -5.3$ to $+1.3$) along with partial melt modeling indicates that the basalts were likely derived from a spinel peridotite source. In contrast, samples collected from the western side (PJ4) of the Kashmir Valley (Buta Pathri) are more primitive in composition and show evidence for clinopyroxene fractionation. The basalts from the western side of the Kashmir Valley have higher Mg# (Mg# = 60 to 78) values and $\varepsilon_{Nd}(t)$ values ($\varepsilon_{Nd}(t) = +0.3$ to $+4.3$) suggesting they were derived by slightly higher amounts of partial melting and from a more depleted spinel peridotite source. The changing bulk composition of the basalts from 'enriched OIB-like' on the eastern side to 'depleted MORB-like' compositions on the western side is likely due to the changing nature of the Panjal rift from a nascent continental setting to one transitioning to a mature ocean basin. In comparison to Pangaean and post-Pangaean flood basalt provinces, the Panjal Traps are more chemically similar to the flood basalts from the post-Pangaean provinces that are associated with plate separation.

Key words: Himalaya, large igneous province, continental flood basalts, Pangaea, India, Early Permian

INTRODUCTION

Flood basalts from continental large igneous provinces (LIPs) represent large scale transfer of mantle material to the crust and reflect prevailing local tectonothermal conditions at the time of their eruption (Coffin and Eldholm, 1994; Jerram and Widdowson, 2005; Saunders and others, 2007; Bryan and Ernst, 2008; Bryan and Ferrari, 2013). Many Phanerozoic LIPs (for example, Karoo, Parana-Etendeka, Deccan, Central Atlantic Magmatic Provinces) are associated with continental break-up

* National Taiwan Normal University, Department of Earth Science, 88 Tingzhou Road Section 4, Taipei 116, Taiwan
** University of Jammu, Department of Geology, Jammu and Kashmir State, India
*** Academia Sinica Institute of Earth Sciences, 128 Academia Road Section 2, Taipei, Taiwan 115
§ Department of Environmental, Earth and Ocean Sciences, University of Massachusetts at Boston, 100 Morrissey Boulevard, Boston, Masschusetts 02125 U.S.A.
§§ National Taiwan University, Department of Geosciences, P.O. Box 13-318, Taipei, Taiwan 106
† Corresponding author: E-mail: jgshelln@ntnu.edu.tw

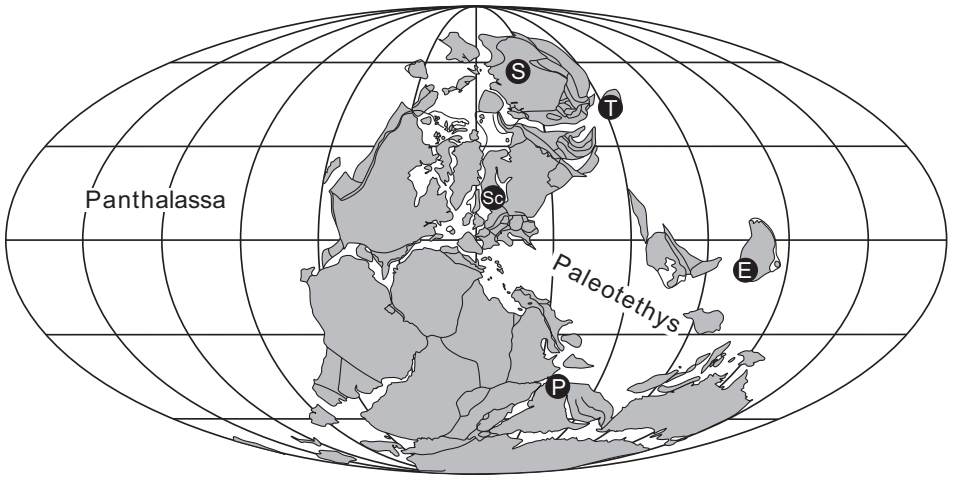

Fig. 1. Early Permian (290 Ma) palaeogeographic reconstruction showing the location of the Panjal Traps (P), Siberian Traps (S), Emeishan large igneous province (E), Skagerrak-Centered LIP (Sc) and Tarim (T) large igneous province (modified from Torsvik and others, 2014).

initiated by either active lithospheric/sublithosperhic processes (mantle plume) or passive lithospheric processes (plate stress field), and mass extinctions (Rampino and Stothers, 1988; Stothers, 1993; Courtillot and others, 1999; Wignall, 2001; Courtillot and Renne, 2003; Ernst and others, 2005; Saunders, 2005; Foulger, 2010). However there are a number of LIPs not associated with continental break-up and/or mass extinctions and many of them occurred during the Late Paleozoic when Pangea was at or near its zenith (Torsvik and others, 2008; Saunders and Reichow, 2009; Shellnutt and others, 2011; Yang and others, 2013; Shellnutt, 2014). There are at least five major eruptions of continental flood basalts during the latest Carboniferous to latest Permian. The emplacement of volcanic and plutonic rocks associated with the Skagerrak-Centered large igneous province (~300 Ma), Himalayan event (~290-270 Ma), Tarim large igneous province (~290-270 Ma), Emeishan large igneous province (~260 Ma) and the Siberian Traps (~251 Ma) cover a combined area of $\sim 2.6 \times 10^6$ km^2 and are mostly composed of mafic volcanic and intrusive rocks (Saunders and others, 2005; Torsvik and others, 2008; Saunders and Reichow, 2009; Zhu and others, 2010; Zhang and others, 2010; Yang and others, 2013; Shellnutt and others, 2014; Shellnutt, 2014).

The Permian aged volcanic rocks within the Himalayan Tethyan domains of Pakistan, India and China are considered to be a magmatic province (Chaudry and Ashraf, 1980; Bhat and others, 1981; Bhat, 1984; Papritz and Rey, 1989; Vannay and Spring, 1993; Spencer and others, 1995; Garzanti and others, 1999; Ernst and Buchan, 2001; Zhu and others, 2010; Shellnutt and others, 2011, 2012, 2014; Ali and others, 2012; Zhai and others, 2013; Wang and others, 2014). The Panjal, Arbor, Nar-Tsum, Bhote Kosi, and Selong volcanic groups and Qiangtang mafic dykes are amongst the many occurrences of Early to Middle Permian basaltic rocks within the Himalaya that are attributed to plate separation and the formation of a new ocean basin (Neotethys/Mesotethys) and the ribbon-like continent Cimmeria (fig. 1; Bhat and others, 1981; Sengor, 1987; Zhu and others, 2010; Shellnutt and others, 2011, 2012, 2014; Ali and others, 2012). It is uncertain if the regionally extensive volcanic rocks are petrogenetically related or if they represent disjointed eruptions within the same regional-scale tensional regime occurring over the first 30 million years of the Permian.

The Panjal Traps of northern India are the largest contiguous outcropping of the Permian (289 ± 3 Ma) Himalayan volcanic groups but they are relatively understudied compared with the other Late Paleozoic flood basalt provinces (Bhat and others, 1981; Chauvet and others, 2008; Shellnutt and others, 2011, 2014). Previous work suggests the Panjal Traps were likely derived by partial melting of an enriched mantle source and represent the epicenter of a continental rift that formed the central Neotethys Ocean whereas others suggest they could be an axial offshoot from a mantle plume centered within the Qiangtang block (Chauvet and others, 2008; Shellnutt and others, 2011, 2014; Zhai and others, 2013). The precise reason (exploitation of a structural heterogeneity) or mechanism (mantle plume vs. lithospheric extension) for the formation and propagation of the rift is not constrained. Furthermore, the eastern and western mountain ranges that surround the Kashmir Valley are composed mainly of Panjal Traps; however nearly all of the available studies focus on the eastern side of the Valley primarily due to accessibility and exposure. Consequently very little is known about the rocks from the western side of the Kashmir Valley or the correlative units in Pakistan (Chaudry and Ashraf, 1980; Papritz and Rey, 1989; Spencer and others, 1995).

Flood basalts from some LIPs (Emeishan large igneous province; Parana) show chemical diversity which is often correlative with areal distribution, time, crust/magma interactions and mantle source evolution (Peate, 1997; Shellnutt, 2014). Therefore it is important to identify the extent of compositional diversity within flood basalts of LIPs so that a complete understanding of their petrogenetic evolution and possible relationships to other geological events such as mass extinctions, continental growth and mineral deposits can be evaluated. For this study we present new major and trace elemental data and whole rock Sr-Nd isotope data for samples collected from both sides of the Kashmir Valley to determine if there is evidence for regional or temporal compositional variation. Additionally we compare the mafic Panjal Traps to flood basalts from Late Palaeozoic to Early Palaeogene continental large igneous provinces in order to investigate the chemo-temporal compositions of volcanic rocks from plate separation and non-plate separation tectonic settings.

Geological background

The Tethyan domain of the Indian Himalaya is composed of Precambrian to Late Paleozoic passive margin sequences that form part of the Higher Himalaya (Nakazawa and others, 1975; Fuchs, 1987; Garzanti and others, 1992, 1994, 1996a, 1996b; Brookfield and others, 2013). The basement rocks are characterized as Precambrian augengranite-gneisses, nebulitic migmatites, gray and dark paragneisses and are known as the Central Crystalline rocks. Overlying the Central Crystalline rocks are the Cambrian argillaceous to arenaceous sedimentary rocks (sandstones, siltstones, shales) of the Phe Formation which are intruded by granites of Late Cambrian age (495 ± 16 Ma). Overlying the Phe Formation is the Upper Cambrian Karsha Formation which consists of a lower unit of slates, siltstones and arkoses followed by carbonate rocks and then an upper unit of slates, siltstones, sandstones and quartzites (Fuchs, 1987). The Upper Cambrian Kurgiakh Formation (shale and sandstone) conformably overlies the Karsha Formation and is uncomformably covered by the Ordovician Thaple Formation (conglomerates, quartzites, sandstones, carbonate sandstones, slates) (Gaetani and others, 1986; Fuchs, 1987; Myrow and others, 2006). The Silurian Muth Quartzite is deposited on top of the Thaple Formation followed by the Lower Carboniferous Lipak Formation (predominantly carbonate rocks and evaporates) and the Middle to Upper Po Formation (shale and quartzites). The Middle to Upper Carboniferous Fenestella Shale (*Spirifer varuna* and *Camarophoria*-bearing) is found just beneath Agglomeratic slate, a mixture of siliciclastic and volcaniclastic rocks, and is followed by

the main eruptive sequence of the Panjal Traps (Nakazawa and others, 1975; Garzanti and others, 1998). The Panjal Traps are up to 3 km in thickness (Kashmir Valley), show evidence of subaerial and subaqueous eruptive environments and are interpreted to have erupted within a coastal or lagoonal environment (Wadia, 1961; Nakazawa and Kapoor, 1973; Nakazawa and others, 1975; Pareek, 1976). There are reports of intertrappean limestones, shales and slates near Gulmarg and Bren but were not observed during this study. The Traps are palaeonotologically constrained to an Upper Permian eruption age by the presence of *Gangamopteris* beds deposited on the Panjal Traps which are followed by sandstones and carbonates of the Zewan Formation and the shales of the Uppermost Permian-Lower Triassic Khunamuh Formation (Nakazawa and others, 1975; Brookfield and others, 2013). The sedimentary rocks were deposited during the Late Paleozoic as a response to differential uplift of the Indian margin during rifting of the ribbon-like continent Cimmeria (Sengor, 1984, 1987; Vannay and Spring, 1993; Garzanti and others, 1999). The eruption of the Panjal Traps, Abor basalts and andesites, the Nar-Tsum spilites and the Bhote Kosi basalts of the eastern and central Himalaya during the Early Permian is evidence that rifting was associated with magmatism and the formation of the Neotethys Ocean although there is debate regarding the role of the Abor volcanics (Bhat and others, 1981; Bhat, 1984; Garzanti and others, 1999; Shellnutt and others, 2011, 2014; Ali and others, 2012).

The Panjal Traps cover an area of $\sim 10^4$ km^2 exposed along the Pir Panjal and Zanskar mountain ranges within the state of Jammu and Kashmir and are continuous into Pakistan (fig. 2). They were first documented in 1824 and named by Lydekker (1883). Detailed structural, stratigraphic and geochronological studies constrained their eruption to the Early Permian (Middlemiss, 1910; Wadia, 1961; Nakazawa and others, 1975; Shellnutt and others, 2011). The Panjal Traps are mostly flood basalts with minor volumes of basaltic andesite, andesite, rhyolite and dacite (Ganju, 1944; Nakazawa and Kapoor, 1973; Pareek, 1976; Bhat and others, 1981; Shellnutt and others, 2012, 2014). The basalts show chemostratigraphic variation as some profiles show distinct changes in TiO_2 (wt.%) content from top to bottom (Shellnutt and others, 2014). Some basalt sequences around the Kashmir Valley show pillow structures whereas at Chandanwadi (~12 km to the northeast of Pahalgam) these show relict columnar joints indicating that the basalt eruptions likely occurred in both subaqueous and subaerial environments (Pareek, 1976; Nakazawa and others, 1975; Bhat and Zainuddin, 1979). The thickness of the flood basalts is reported to range from ~3 km in the Pir Panjal Range to ≤ 0.3 km in the Zanskar Range with individual flow thickness up to 30 m (Middlemiss, 1910; Wadia, 1934; Fuchs 1987; Chauvet and others, 2008). The Panjal volcanic center was likely located in western Kashmir (Kashmir Valley) because the total flow thickness is the thickest in that region (Nakazawa and Kapoor, 1973). Basaltic andesites and andesites were identified specifically within the high-Ti flood basalt segments of the Guryal Ravine section in the Kashmir Valley (Shellnutt and others, 2014). The silicic volcanic rocks (dacites and rhyolites) are only found underlying the basalt flows within the Kashmir Valley and are interpreted to represent crustal melts (Ganju, 1944; Shellnutt and others, 2012). Komatiitic rocks located at Chhongtash in northern Ladakh are tentatively correlated with the Panjal Traps but their precise association remains uncertain (Rao and Rai, 2007).

The rocks collected for this study were located at two different sites (PJ3 and PJ4) within the Kashmir Valley (fig. 2). Six samples (PJ3) were collected from the eastern side of the Kashmir Valley located ~1 km south of the town of Batagund which is ~50 km ESE of Srinagar. The samples were collected in two groups. The first group (33°56′41.58′′N, 75°5′31.98′′E) consists of samples PJ3-002, -003, -004, 005A and-005B

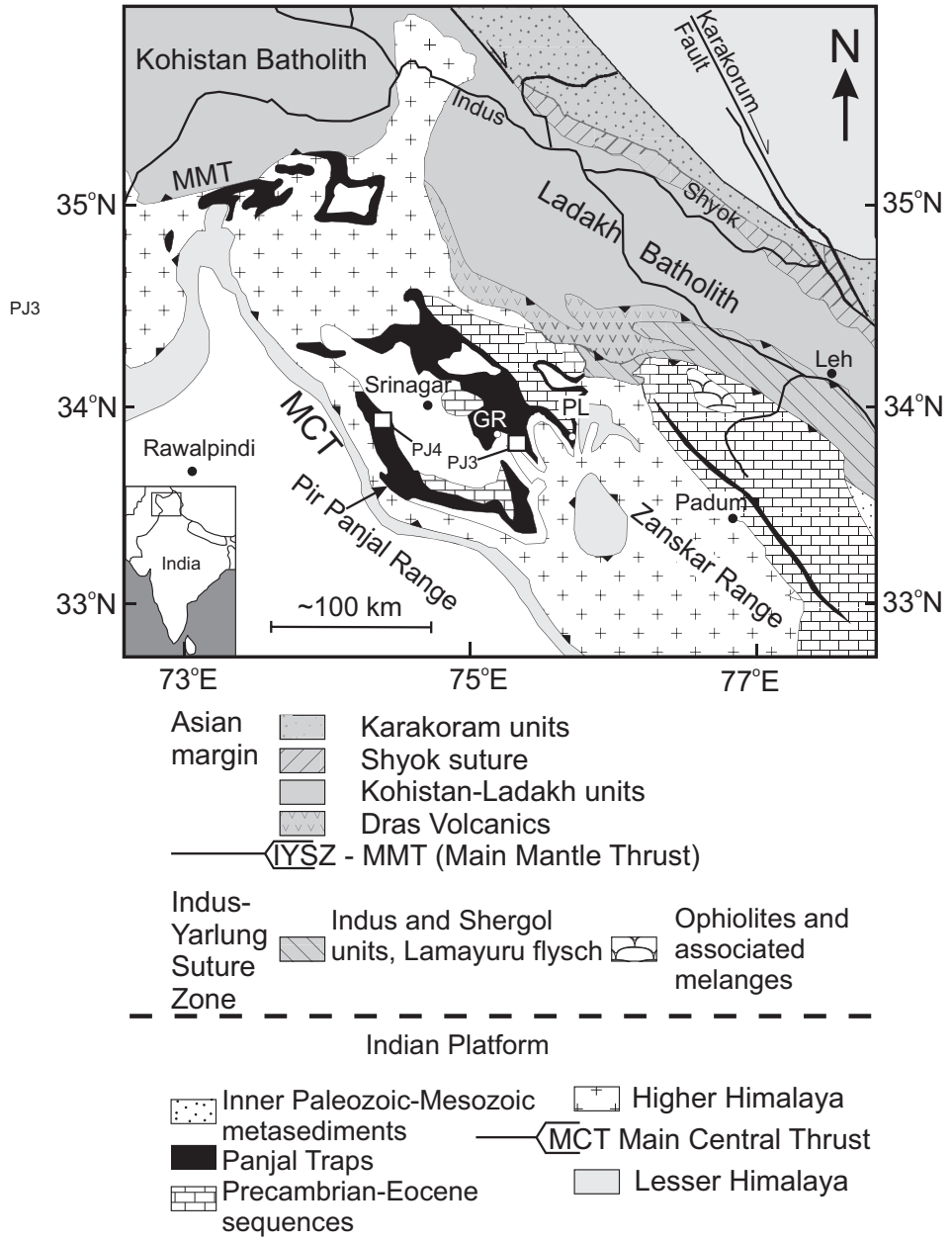

Fig. 2. Geological map of northern India showing the location of the Panjal Traps (black) and the sampling localities at Guryal Ravine (GR), Pahalgam (PL), PJ3 and PJ4 (modified from Chauvet and others, 2008).

whereas sample PJ3-006 (33°55′57.9′′N, 75°4′53.16′′E) was collected ~1.7 km to the southwest of the first group. The rocks are fine grained and have experienced lower greenschist facies metamorphism as many of the original mafic minerals have been replaced with chlorite/amphibole or serpentine whereas the relict, lath-like plagio-

clase textures are still visible. The original microcrystalline seriate texture is preserved and the rocks may be described as spilites without amygdules. An additional seven samples (PJ4) were collected on the western side of the Kashmir Valley within the Pir Panjal range in the Buta Pathri area, ~30 km west of Srinagar. Samples were taken from the base of the mountain (33°58′47.76′′N, 74°30′32.16′′E) to ~500 m up slope (33°58′55.8′′N, 74°30′6.78′′E) of a river cutting starting from PJ4-001 at the base to PJ4-008 at the 500 m interval. Similar to the PJ3 samples, the PJ4 samples have experienced lower greenschist metamorphism but the relict rock textures are more porphyritic with larger phenocrysts within a finer-grained matrix. The original mafic phenocrysts and matrix minerals have not been preserved but based on the textures and alteration products (chlorite, serpentine) it appears the phenocrysts could have been olivine whereas the matrix was primarily composed of nearly equal proportions of plagioclase and clinopyroxene.

ANALYTICAL METHODS

Wavelength Dispersive X-ray Fluorescence Spectrometry

Rock samples were cut into small pieces using a diamond-bonded steel saw and were then crushed in a steel jaw crusher. The crusher was extensively cleaned after each sample with de-ionized water. The crushed samples were pulverized in an agate mill until the suitable particle size was obtained. After drying at 110 °C the samples were heated to 900 °C to determine loss on ignition (LOI). Lithium metaborate was added to the oxidized samples and fused to produce a glass disc using a Claisse M4 fluxer. The major oxide concentrations were determined by WD-XRFS using a PANalytical Axios mAX spectrometer at National Taiwan Normal University in Taipei. The long term precision for SDC-1 standard reference material on >30 analyses is better than ± 0.5 percent on all elements except MgO, Na_2O and P_2O_5 which are better than ± 2 percent (table 1). The long term precision for BIR-1 standard reference material on >39 analyses is better that ± 0.5 percent on all elements except Na_2O and K_2O which are ± 2 percent (table 1).

ICP-MS Trace Element Geochemistry

Whole rock trace elemental analysis was conducted at Activation Laboratories, Ancaster, Ontario, Canada using their total digestion ICP method. The detailed sample methods and preparation techniques can be found on the Activation Laboratories website and are summarized below. A 0.25 g sample is digested with four acids beginning with hydrofluoric, followed by a mixture of nitric and perchloric acids. The solution is then heated through several ramping and holding cycles to incipient dryness. The dried samples are then brought back into solution using aqua regia. The solutions are analyzed using an Agilent 735 inductively coupled plasma mass spectrometer. Quality control for the digestion is reported to be 14 percent for each batch using 5 method reagent blanks, 10 in-house controls, 10 samples duplicates, and 8 certified reference materials. The results can be found in table 1.

TIMS Rb-Sr and Sm-Nd Isotopic Analyses

Approximately 75 to 100 mg of whole-rock powder of each sample was dissolved using a mixture of HF-$HClO_4$ in a Teflon beaker at ~100 °C. In many cases, the same procedures were repeated to ensure the total dissolution of the sample. Strontium and REEs were separated using polyethylene columns with a 5 ml resin bed of AG 50W-X8, 200 to 400 mesh. Neodymium was separated from other REEs using polyethylene columns with a Ln resin as a cation exchange medium. Strontium was loaded on a single Ta-filament with H_3PO_4 and Nd was loaded with H_3PO_4 on a Re-double-filament. The $^{143}Nd/^{144}Nd$ ratios were normalized to $^{146}Nd/^{144}Nd = 0.7219$ and

TABLE 1

Major and trace element data of the mafic Panjal Traps

Sample	PJ3-002	PJ3-003	PJ3-004	PJ3-005A	PJ3-005B	PJ3-006	PJ4-001	PJ4-003	PJ4-004	PJ4-005
SiO_2 (wt.%)	51.93	50.30	50.65	50.26	46.06	44.60	48.08	56.36	39.55	50.14
TiO_2	0.94	0.96	0.90	0.95	1.45	0.90	1.02	0.90	0.92	1.03
Al_2O_3	14.86	15.01	13.47	14.43	15.98	14.06	14..25	14.48	11.32	16.55
Fe_2O_3t	9.04	9.60	9.26	9.98	12.36	10.05	10.82	8.91	11.99	9.86
MnO	0.11	0.14	0.15	0.15	0.19	0.17	0.19	0.15	0.20	0.12
MgO	7.63	4.79	8.57	9.06	7.89	9.27	10.30	5.57	21.18	7.36
CaO	8.19	9.92	7.50	7.81	7.49	8.67	7.54	8.58	6.48	7.00
Na_2O	1.41	1.42	1.45	1.43	2.87	2.50	2.56	2.08	0.05	3.27
K_2O	0.30	0.37	0.55	0.65	0.09	0.50	0.38	0.17	0.02	0.64
P_2O_5	0.09	0.11	0.08	0.09	0.12	0.06	0.07	0.09	0.07	0.10
LOI	5.42	7.75	7.23	4.84	5.17	8.45	4.46	2.98	6.87	3.35
Total	99.92	100.36	99.81	99.65	99.67	99.23	99.67	100.27	98.65	99.42
Mg#	62.6	49.7	64.7	64.3	55.8	64.6	65.3	55.3	77.8	59.7
V (ppm)	198	195	207	195	200	262	251	228	227	264
Cr	340	210	250	510	520	290	540	470	1240	2080
Co	37	37	39	42	45	53	45	34	64	46
Ni	120	80	100	190	200	200	90	190	430	310
Cu	70	60	90	70	100	130	20	90	30	100
Zn	70	80	80	80	80	100	80	80	90	100
Ga	17	18	18	16	17	19	15	19	14	17
Rb	16	20	29	21	23	3	14	10	b.d.	26
Sr	177	185	143	276	296	98	74	93	8	97
Y	23.0	23.1	23.7	22.4	22.9	28.4	19.6	22.1	14.4	18.9
Zr	86	94	96	89	92	115	61	101	50	49
Nb	10.5	9.9	9.7	8.2	8.1	8.6	4.3	6.7	3.4	3.1
Cs	1.0	1.1	1.9	1.3	1.1	0.3	1.0	0.7	0.2	0.8
Ba	86	74	197	247	291	74	128	25	b.d	84
La	14.2	13.9	15.2	13.1	12.9	15.2	7.59	17.1	2.22	5.11
Ce	28.8	29.1	20.8	26.9	27.1	30.7	16.7	34.8	5.83	11.5
Pr	3.46	3.44	3.66	3.25	3.29	3.77	2.15	4.02	0.90	1.62
Nd	14.1	13.9	15.2	13.6	13.5	15.2	9.68	16.2	4.29	7.41
Sm	3.55	3.39	3.81	3.27	3.21	4.04	2.54	3.52	1.50	2.25
Eu	0.90	0.93	1.05	0.87	0.87	1.55	0.76	0.83	0.34	0.81
Gd	3.55	3.61	4.06	3.25	3.46	4.25	3.04	3.51	2.05	2.81
Tb	0.60	0.63	0.67	0.58	0.60	0.74	0.53	0.61	0.38	0.49
Dy	3.72	3.79	4.08	3.73	3.71	4.65	3.37	3.69	2.50	3.11
Ho	0.75	0.77	0.81	0.73	0.76	0.98	0.69	0.75	0.54	0.67
Er	2.20	2.19	2.32	2.21	2.24	2.85	2.01	2.27	1.60	1.94
Tm	0.32	0.33	0.34	0.32	0.33	0.41	0.29	0.34	0.24	0.28
Yb	2.05	2.01	2.13	2.01	2.04	2.59	1.79	2.14	1.57	1.80
Lu	0.32	0.32	0.32	0.31	0.30	0.39	0.27	0.33	0.24	0.27
Hf	2.4	2.5	2.6	2.3	2.3	3.0	1.7	2.7	1.4	1.3
Ta	0.51	0.59	0.60	0.49	0.48	0.52	0.25	0.56	0.21	0.20
Th	4.28	4.47	4.63	4.06	4.18	3.81	2.00	5.81	1.12	1.09
U	1.00	1.11	1.17	0.78	0.84	0.71	0.33	1.30	0.23	0.26
$(La/Yb)_N$	4.9	4.9	5.1	4.6	4.5	4.2	3.0	5.7	1.0	2.0
Eu/Eu*	0.76	0.79	0.80	0.80	0.78	1.12	0.83	0.70	0.59	0.97

TABLE 1
(Continued)

Sample	PJ4-006	PJ4-007	PJ4-008	PJ-008 (dup)	DNC-1 m.y.	DNC-1 r.v	BIR m.y.	BIR r.v.	W-12a m.y.	W-12a r.v.
SiO_2 (wt.%)	52.14	47.08	48.70				47.75	47.96		
TiO_2	0.98	0.92	0.86				0.96	0.96		
Al_2O_3	12.37	13.11	12.18				15.42	15.5		
Fe_2O_3t	8.69	10.62	9.34				11.16	11.3		
MnO	0.15	0.15	0.15				0.17	0.175		
MgO	7.37	10.94	12.29				9.59	9.70		
CaO	11.90	10.38	9.72				13.22	13.3		
Na_2O	3.25	1.93	2.35				1.73	1.82		
K_2O	0.43	0.33	0.17				0.03	0.03		
P_2O_5	0.07	0.07	0.06				0.02	0.21		
LOI	2.27	3.78	3.98				-0.28			
Total	99.62	99.31	99.80				99.78			
Mg#	62.7	67.1	72.3							
V (ppm)	220	235	206	210	145	148			269	262
Cr	780	1270	1040	1060					90	92
Co	34	47	45	44	63	57	56	52	43	43
Ni	170	420	430	420			180	170	70	70
Cu	100	120	80	80	110	100	130	125	100	110
Zn	60	70	60	60						
Ga	12	15	12	12			17	16	17	17
Rb	13	11	5	5					19	21
Sr	66	146	131	132			119	110	197	190
Y	17.9	17.0	16.8	17.0	18.3	18.0	16	16		
Zr	46	45	42	40					95	94
Nb	2.7	2.5	2.2	2.3					8.5	7.9
Cs	0.5	0.5	0.3	0.4						
Ba	71	70	38	40	110	118			155	182
La	4.81	4.34	3.88	4.15					10.3	10.
Ce	10.7	10.1	8.85	9.42					22.5	23
Pr	1.46	1.41	1.28	1.39						
Nd	6.94	6.63	6.37	6.26	5.17	5.20	2.66	2.5	12.2	13
Sm	2.13	2.10	1.93	1.98			1.16	1.1	3.12	3.3
Eu	0.80	0.73	0.85	0.84			0.56	0.55	1.02	1
Gd	2.67	2.44	2.46	2.52			2	2.0		
Tb	0.48	0.45	0.45	0.44						
Dy	3.03	2.88	2.84	2.83					3.59	3.6
Ho	0.62	0.60	0.58	0.58					0.74	0.76
Er	1.80	1.72	1.70	1.68						
Tm	0.27	0.26	0.24	0.25						
Yb	1.71	1.68	1.50	1.59	2.02	2.0	1.78	1.7	1.92	2.1
Lu	0.26	0.25	0.22	0.24						
Hf	1.3	1.3	1.2	1.2			0.6	0.6	2.4	2.6
Ta	0.19	0.19	0.19	0.18					0.49	0.5
Th	0.84	0.74	0.71	0.77						
U	0.22	0.20	0.37	0.37					0.55	0.53
$(La/Yb)_N$	2.0	1.8	1.8							
Eu/Eu*	1.00	0.97	1.18							

LOI = loss on ignition; Mg# = $[Mg^{2+}/(Mg^{2+}+Fe^{2+})]*100$; FeO = $0.8998*Fe_2O_3t$; N = normalized to chrondite values of Sun and McDonough (1989); Eu/Eu* = $[2*Eu_N/(Sm_N+Gd_N)]$. dup = duplicate. m.v. = measured value, r.v. = recommended value. b.d. = below detection limit.

$^{87}Sr/^{86}Sr$ ratios to $^{86}Sr/^{88}Sr = 0.1194$. The Sr isotopic ratios were measured using a Finnigan MAT-262 thermal ionization mass spectrometer (TIMS) whereas the Nd isotopic ratios were measured using a Finnigan Triton TIMS in the Mass Spectrometry Laboratory, Institute of Earth Sciences, Academia Sinica, Taipei. The $2\sigma_m$ values for all samples are less than or equal to 0.000014 for $^{87}Sr/^{86}Sr$ and less than or equal to 0.000007 for $^{143}Nd/^{144}Nd$ (table 2). The measured isotope ratio for JMC Nd standard is 0.511813 ± 0.000010 ($2\sigma_m$) and NBS987-Sr is 0.710248 ± 0.00001 ($2\sigma_m$). The results can be found in table 2.

RESULTS

Major and Trace Elemental Geochemistry

The basalts from section PJ3 are mildly alkalic to tholeiitic in composition and have Mg# values ($Mg\# = [Mg^{2+}/[Mg^{2+}+Fe^{2+}]]*100$) of 50 to 65 (figs. 3A and 3B). The concentration of MgO (4.8–9.3 wt%) and CaO (7.5–9.9wt%) are variable between all samples but PJ3-006 is noticeably different with higher TiO_2 (1.5 wt%), Fe_2O_3t (12.4 wt%) and Al_2O_3 (16.0 wt%) (fig. 3). The loss on ignition (LOI) values are high and range between 4.5 and 8.5 weight percent indicating the rocks were metamorphosed.

The basaltic rocks from section PJ4 are more 'primitive' than those from PJ3. The MgO contents range from 7.4 to 21.2 weight percent with Mg# values between 62 and 77 and SiO_2 between 39.6 and 52.1 (Fig. 3B). The PJ4 basalts tend to have higher total alkalis ($Na_2O+K_2O = 0.1$ to 3.9 wt%) and lower Al_2O_3 (11.3 to 16.6 wt%) than those from PJ3 whereas CaO (6.5–11.9 wt%) is more variable and Fe_2O_3t (8.7–10.8 wt%), TiO_2 (0.9–1.0 wt%) and P_2O_5 (≤ 0.1 wt%) are about the same. The LOI is high for most samples and ranges from 2.3 and 6.9 weight percent. Sample PJ4-004 has significantly higher MgO and lower total alkalies which probably reflect the presence of olivine psuedomorphs. Sample PJ4-003 is the lone basaltic andesite in this study but is compositionally similar to the basaltic andesites described from previous studies (Shellnutt and others, 2014).

The bulk trace element compositions of the PJ3 and PJ4 basaltic rocks match the compositional difference observed with their major element compositions. For example, the Mg# of the PJ3 samples is generally lower than PJ4 as are many of the transition metals (PJ3 V = 195–262 ppm, Cr = 210–520 ppm, Co = 37–53 ppm, Ni = 80–200 ppm; PJ4 V = 208–264 ppm, Cr = 470-2080 ppm, Co = 34–64 ppm, Ni = 90–430 ppm). Furthermore the high field strength elements (PJ3 Zr = 86–115 ppm, Nb = 8.1–10.5 ppm, Hf = 2.3–3.0 ppm, Ta = 0.48–0.60 ppm, Th = 4.1–4.6 ppm, U = 0.7–1.1 ppm; PJ4 Zr = 41–61 ppm, Nb = 2.2–4.3 ppm, Hf = 1.2–1.7 ppm, Ta = 0.2–0.6 ppm, Th = 0.7–2.0 ppm, U = 0.2–0.4 ppm) and large ion lithophile elements (Cs, Rb, Ba and Sr) tend to be lower in the PJ4 samples for the exception of Rb (PJ3 Rb = 3–29 ppm; PJ4 Rb $\leq$ 26) but may reflect element mobility during metamorphism.

The primitive mantle normalized incompatible trace element patterns reveal some differences between the two groups of rocks. The PJ3 samples tend to be more enriched overall than the PJ4 samples in particular the most incompatible elements (fig. 4A). Perhaps the most obvious difference between the two groups is the higher concentration of Th, U, Nb and Ta in the PJ3 samples in comparison to the PJ4 samples. The remaining elements show similar patterns with the exception of the Sr depletion within sample PJ4-004. The chondrite normalized REE patterns are very similar between the PJ3 samples but the PJ4 samples show variability in the light rare earths ($La/Sm_N = 0.9$ to 1.9) whereas the middle and heavy rare earth elements are more uniform and flat ($Gd/Lu_N = 1.0–1.2$). The Eu-anomalies, as defined by Eu/Eu*, are mostly between 0.7 and 1.0 but sample PJ4-004 is noticeably lower (0.6) and PJ4-008 is higher (1.2) (fig. 4B).

TABLE 2

Whole rock Sr and Nd isotope data of the Panjal Traps

Sample	Rock	Rb (ppm)	Sr (ppm)	$\frac{^{87}Rb}{^{86}Sr}$	$\frac{^{87}Sr}{^{86}Sr}$	$\pm 2\sigma_m$	I_{Sr}	Sm (ppm)	Nd (ppm)	$\frac{^{147}Sm}{^{144}Nd}$	$\frac{^{143}Nd}{^{144}Nd}$	$\pm 2\sigma_m$	$\varepsilon Nd_{(0)}$	$\varepsilon Nd_{(T)}$	f (Sm/Nd)	T_{DM}-1
PJ3-002	Basalt	16	177	0.262	0.71432	9	0.71325	3.55	14.1	0.1522	0.51235	6	-5.6	-3.9	-0.23	1973
PJ3-004	Basalt	18	143	0.364	0.71508	9	0.71358	3.81	15.2	0.1515	0.51237	6	-5.2	-3.6	-0.23	1911
PJ3-005A	Basalt	16	276	0.168	0.71373	13	0.71304	3.27	13.6	0.1454	0.51237	7	-5.2	-3.3	-0.26	1733
PJ3-005B	Basalt	17	296	0.166	0.71380	11	0.71312	3.21	13.5	0.1438	0.51241	6	-4.4	-2.5	-0.27	1609
PJ3-006	Basalt	3	98	0.089	0.71219	8	0.71183	4.04	15.2	0.1607	0.51238	6	-5.0	-3.7	-0.18	2199
PJ4-001	Basalt	14	74	0.548	0.71947	9	0.71722	2.54	9.68	0.1586	0.51258	6	-1.1	+0.3	-0.19	1577
PJ4-003	Andesite	10	93	0.311	0.71453	7	0.71325	3.52	16.2	0.1314	0.51216	5	-9.3	-6.8	-0.33	1819
PJ4-004	Basalt							1.50	4.29	0.2114	0.51279	6	+3.0	+2.4	+0.07	2224
PJ4-005	Basalt	26	97	0.776	0.71126	11	0.70807	2.25	7.41	0.1836	0.51278	7	+2.8	+3.2	-0.07	1891
PJ4-006	Basalt	13	66	0.570	0.71088	9	0.70854	2.13	6.94	0.1855	0.51282	6	+3.6	+3.9	-0.06	1807
PJ4-007	Basalt	11	149	0.214	0.71204	8	0.71116	2.10	6.63	0.1915	0.51284	6	+3.9	+4.2	-0.03	2092
PJ4-008	Basalt	5	132	0.110	0.71282	9	0.71236	1.95	6.32	0.1865	0.51284	6	+3.9	+4.3	-0.05	1736

Rb, Sr, Sm and Nd concentrations were obtained by ICP-MS and precisions better than ±2%. The results of isotopic measurements for Sr and Nd reference materials are NBS-987 (Sr) = 0.710248 ± 3 (2σm). JMC (Nd) = 0.511813 ± 10 (2σm). f(Sm/Nd) is defined as $(({}^{147}Sm/{}^{144}Nd)/0.1967\text{-}1)$. $\varepsilon Nd_{(T)}$ is calculated using an approximate equation of $\varepsilon Nd_{(T)} = \varepsilon Nd_{(0)}\text{-}Q*f*T$; in which Q = 25.1 Ga^{-1}, f = f(Sm/Nd), T age = 0.289 Ga. T_{DM}-1 = $(1/\lambda)*\ln[1+(({}^{143}Nd/{}^{144}Nd)_m\text{-}0.51315)/(({}^{147}Sm/{}^{144}Nd)_m\text{-}0.2137)]$; $\lambda = 0.00654\ Ga^{-1}$.

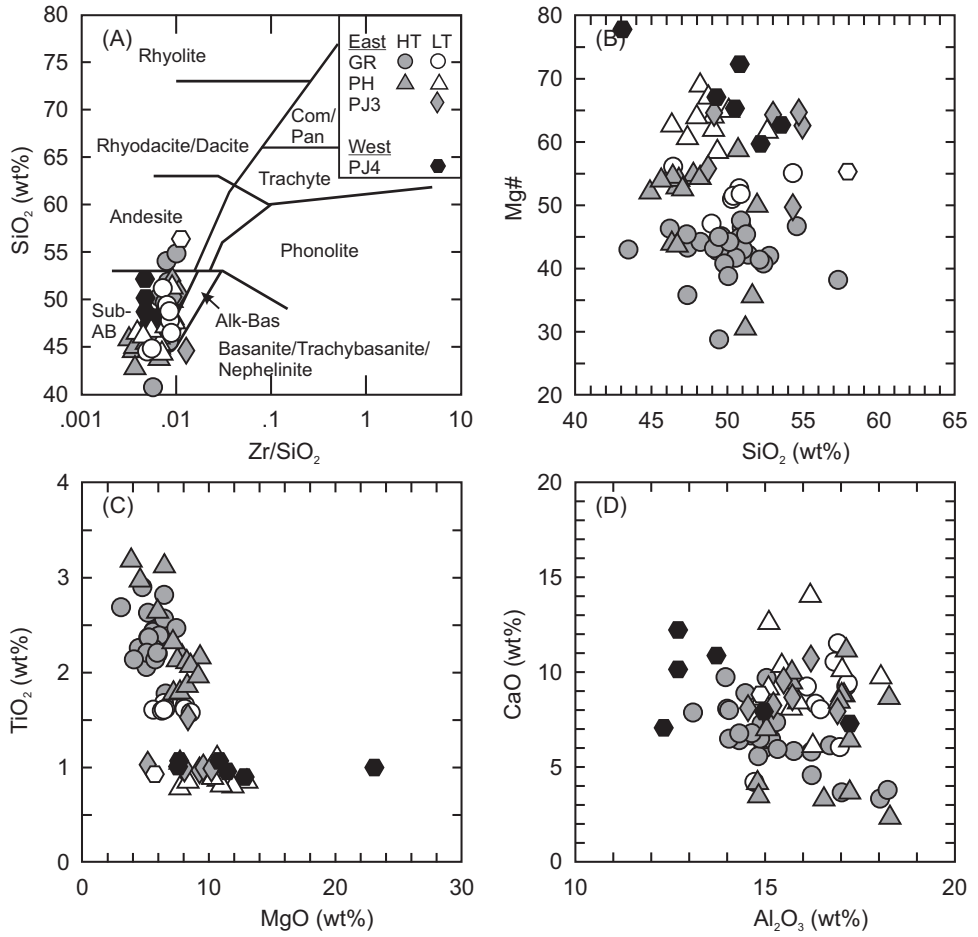

Fig. 3. (A) Rock classification of Winchester and Floyd (1977) using immobile elements of the mafic Panjal Traps. Sub-AB = subalkaline basalts, Alk-Bas = alkaline basalt, Com/Pan = Comendite/Pantellerite. (B) Mg# vs. SiO_2 (wt.%), (C) TiO_2 vs. MgO (wt.%) and (D) CaO vs. Al_2O_3 (wt%). Samples from the eastern Kashmir Valley = east, samples from western Kashmir Valley = west. HT = high TiO_2, LT = low-TiO_2. Data are normalized to 100%.

Sr-Nd Isotope Geochemistry

The Sr-Nd isotope analyses are calculated using the 289 Ma U/Pb age reported from the silicic Panjal Traps (table 2). The initial $^{87}Sr/^{86}Sr$ values are quite high for basaltic rocks ranging from 0.70818 to 0.71366 but the calculated induced error values are all low (< 0.00005). Based on the petrography and high LOI values many of the rocks have experienced greenschist metamorphic conditions that may have influenced the Sr or Rb contents. The initial $^{143}Nd/^{144}Nd$ ratios range from a low of 0.51190 in sample PJ4-003 to a high of 0.51245 in sample PJ4-008 but it is clear that the two groups of samples are different. The PJ3 samples have $\varepsilon_{Nd}(t)$ values between -2.5 and -3.9 whereas the basaltic PJ4 samples range between $+0.3$ and $+4.3$ (fig. 5). Sample PJ4-003 (andesitic) has an $\varepsilon_{Nd}(t)$ of -6.8 which is similar to other Panjal andesitic rocks (Shellnutt and others, 2014). The fractionation factor ratios (f(Sm/Nd)) range from $+0.07$ to -0.27 and the corresponding meaningful T_{DM} values for samples with f(Sm/Nd) between -0.2 and -0.6 ranges from 1580 Ma to 2200 Ma.

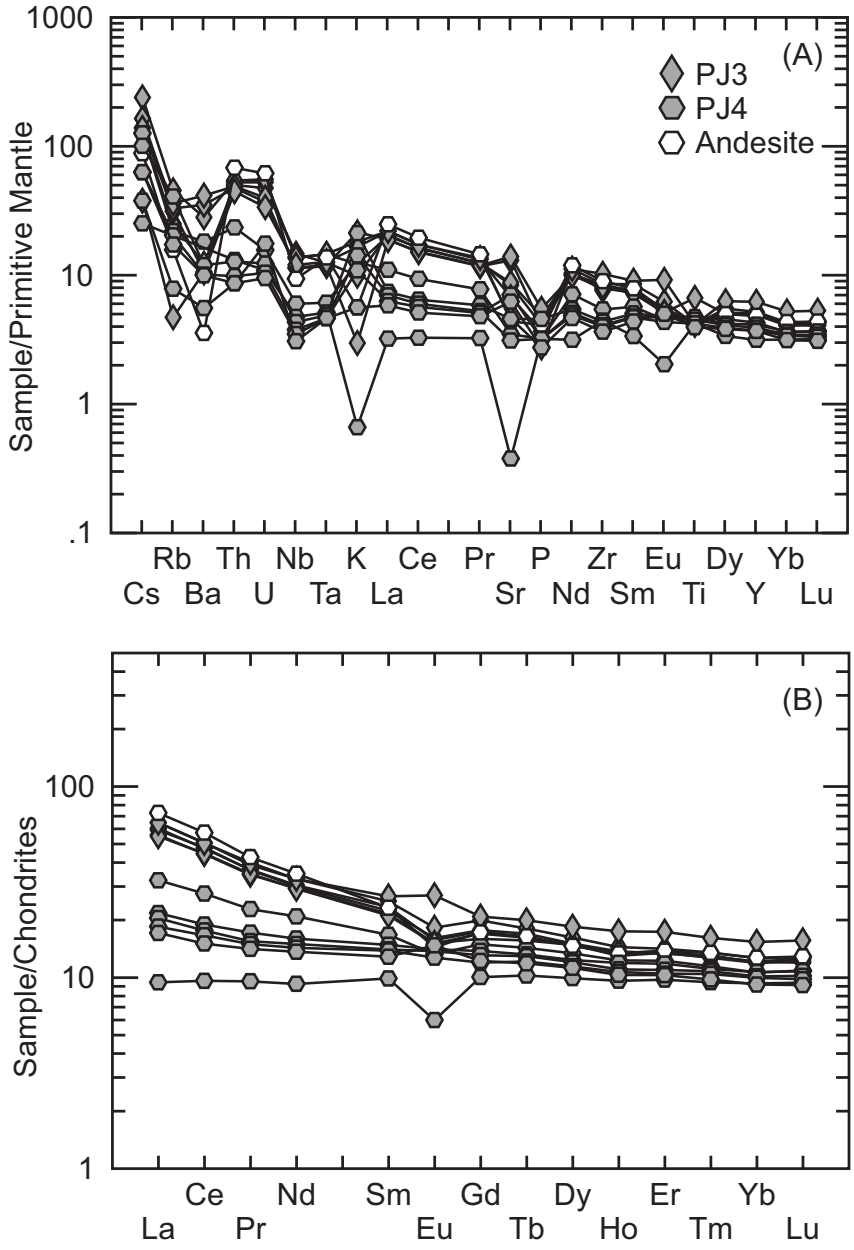

Fig. 4. (A) Primitive mantle normalized incompatible element plot and (B) chondrite normalized rare earth element plot of the mafic rocks of the Panjal Traps from sections PJ3 and PJ4. Samples are normalized to the values of Sun and McDonough (1989).

DISCUSSION

Petrogenetic Controls on the Composition of the Panjal Traps Around the Kashmir Valley

The mafic Panjal Traps are described as within-plate tholeiitic to mildly alkalic basalts that erupted within a continental rift setting (Bhat and Zainuddin, 1979; Bhat

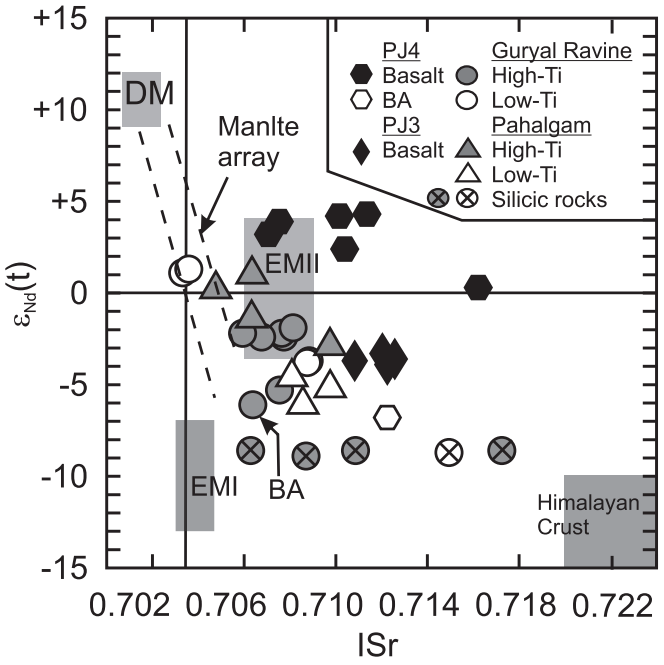

Fig. 5. Sr-Nd plot showing the mafic and silicic Panjal traps from the Kashmir Valley region. BA = basaltic andesite, DM = depleted mantle, EMI = enriched mantle I, EMI = enriched mantle II (Zindler and Hart, 1986; Workman and others, 2004; Workman and Hart, 2005). Isotopic range of the Himalayan crust from Spencer and others (1995).

and others, 1981; Chauvet and others, 2008; Shellnutt and others, 2014). The Traps have light rare earth element enriched ($La/Yb_N \approx 4$) chondrite normalized patterns and classify as 'within-plate basalt' using major and trace elemental tectonomagmatic discrimination diagrams. Partial melt trace-element modeling indicates the mantle source is likely a spinel-bearing lhzerolite (Shellnutt and others, 2014). The low La/Sm and low Sm/Yb_{PM} values of the Panjal Traps, including the PJ3 and PJ4 samples, follow the spinel peridotite melt curve in figure 6. Moreover, a spinel peridotite source is supported by their relatively low Nb/Y ($Nb/Y \leq 0.5$) and Zr/Y ($Zr/Y \leq 4.6$) ratios (Fitton and others, 1997; Baksi, 2001). Although we cannot completely rule out the possibility of garnet in the source it would have to be a very minor (< 1%) constituent. The estimated amount of melting ranges between ~1 percent and ~15 percent for the entire suite of rocks.

The bulk composition and chemostratigraphic variations of TiO_2 observed within the profiles of Guryal Ravine and Pahalgam have shown that the mafic Panjal Traps can be subdivided into high- and low-Ti groups (fig. 3C). The basalts with higher TiO_2 (>1.8 wt%) content are likely derived by lower (~1% to ~5%) amounts of melting compared with the rocks with lower TiO_2 (<1.6 wt%) content that are derived by higher (~10% to ~15%) amounts of melting (Shellnutt and others, 2014). The initial division between the high- and low-Ti groups was not well defined partially due to differences between the Guryal Ravine rocks and the Pahalgam rocks (Shellnutt and others, 2014). For example, at Guryal Ravine the high-Ti group has TiO_2 >1.8 weight percent whereas the low-Ti group has TiO_2 between 1.6 weight percent and 1.4 weight percent. In contrast, the low-Ti basalts at Pahalgam have ≤ 1.0 weight percent TiO_2 but the high-Ti basalts are approximately the same as those from Guryal Ravine. Figure 7A

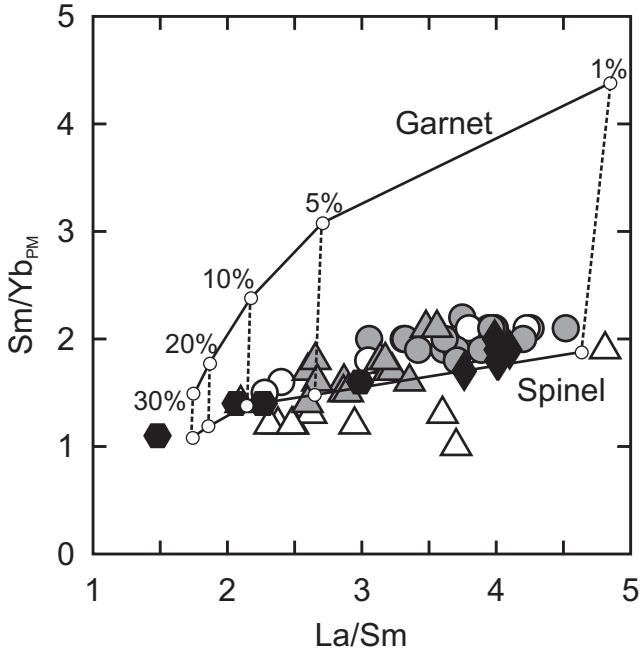

Fig. 6. Trace elemental partial melting modeling showing the primitive mantle normalized Sm/Yb_{PM} ratio vs. La/Sm of a 2% garnet-bearing peridotite (olivine = 57%, opx = 26%, cpx = 15%) and 2% spinel-bearing peridotite. Symbols as in figure 2. Sm/Yb ratio normalized to primitive mantle values of Sun and McDonough (1989). Batch melting equation: $C_L/C_o = 1/D(1\text{-}F)+F$, C_L = concentration in the liquid, C_o = original rock composition, D = bulk distribution coefficient, F = weight fraction of melt produced. Kd values: Y, olivine = 0.005, opx = 0.018, cpx = 0.4, spinel = 0.02, garnet = 7; Sm, olivine = 0.007, opx = 0.05, cpx = 0.26, spinel = 0.01, garnet = 0.102; Yb, olivine = 0.049, opx = 0.227, cpx = 0.166, spinel = 0.01, garnet = 8.5 (Arth, 1976; Irving and Frey, 1978; Fujimaki and others, 1984; Green and others, 1989, 2000; McKenzie and O'Nioins, 1991; Beattie, 1994; Jenner and others, 1994; Johnson, 1994; Salters and Longhi, 1999; Klemme and others, 2006).

shows the classification of the Panjal Traps using the method of Lightfoot and others (1993). The high/low distinction shows rocks from PJ4, PJ3 and the lowest-Ti rocks from Pahalgam are equivalent to 'low-Ti' basalts and have Mg# > 57 whereas the rocks from Guryal Ravine, and the highest-Ti rocks from Pahalgam are equal to 'high-Ti' basalts and have Mg# < 57. The rocks with higher Mg# (>57) values are likely derived by higher amounts of melting or possibly represent higher temperature magmas as these rocks tend to have higher Ni (> 100 ppm) content than the rocks with lower Mg# values (Ni < 100 ppm). Moreover the frequency distribution of the basalts using the Ti/Y ratio, a commonly used discriminator for basalts (Lightfoot and others, 1993; Xu and others, 2001), can distinguish three groups (fig. 7B): 1) the high Ti/Y group (>450), the middle group (Ti/Y >290 and < 450) and the low Ti/Y group (<290). The groupings in figures 7A and 7B are broadly similar but there is a significant difference with respect to the lowest Ti/Y rocks. Figure 7C shows the rocks from PJ4 fall within the middle Ti/Y group whereas only the lowest-Ti Pahalgam and PJ3 rocks form the low Ti/Y group in spite of their similar Mg# values and common 'low-Ti' grouping in figure 7A. The split between the PJ4 samples and the PJ3 and lowest-Ti Pahalgam rocks may reflect differences in the effects of crustal assimilation. In figure 7D the low Ti/Y group has, on average, the lowest $\varepsilon_{Nd}(t)$ values of the mafic Panjal Traps and are trending toward the direction of the silicic Panjal rocks. The silicic rocks are consid-

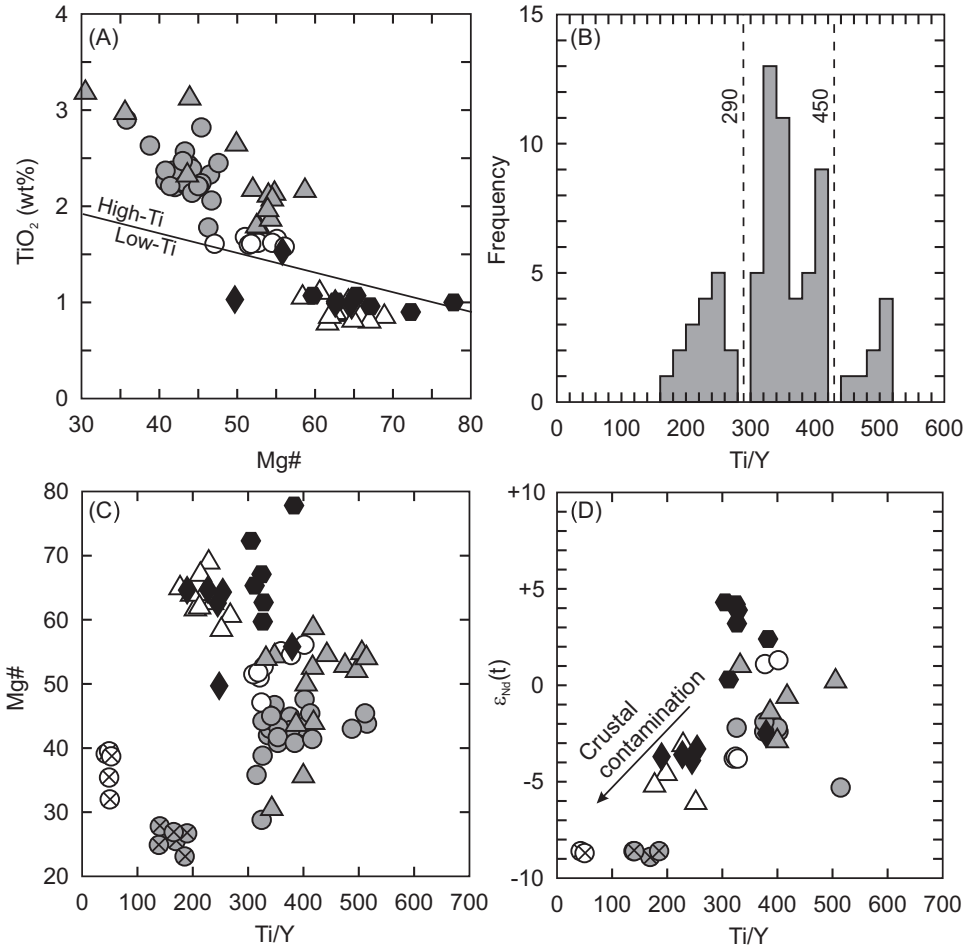

Fig. 7. Ti-classification of the Panjal Traps. (A) TiO_2 (wt%) vs. Mg# (modified from Lightfoot and others, 1993). (B) Ti/Y ratio frequency distribution, (C) Mg# vs. Ti/Y and (D) $\varepsilon_{Nd}(t)$ vs. Ti/Y. Data from this study and Shellnutt and others (2014). Symbols as in figure 5.

ered to be derived by crustal melting and may be a proxy for the isotopic composition of the Himalayan crust (Spencer and others, 1995; Shellnutt and others, 2012). Therefore the Ti classification of the mafic Panjal Traps is somewhat cumbersome and probably reflects differences between the effects of partial melting and crustal assimilation.

Evidence for crystal fractionation in the Panjal Traps was reported in samples from Pahalgam but no other areas (Shellnutt and others, 2014). Pearce element ratios (PER) demonstrate that the high-Ti ($TiO_2 > 1.6$ wt%) basalts from Pahalgam experienced fractionation of olivine and plagioclase. In comparison, the samples from the PJ4 section are consistent with clinopyroxene and olivine fractionation but the PJ3 samples do not show evidence of fractionation of silicate minerals (fig. 8). The difference in the fractionation assemblage between the high-Ti Pahalgam samples and the PJ4 samples is probably related to their original melt composition ('high-Ti' vs. 'low-Ti') where the high-Ti melts fractionate olivine and plagioclase whereas the low-Ti

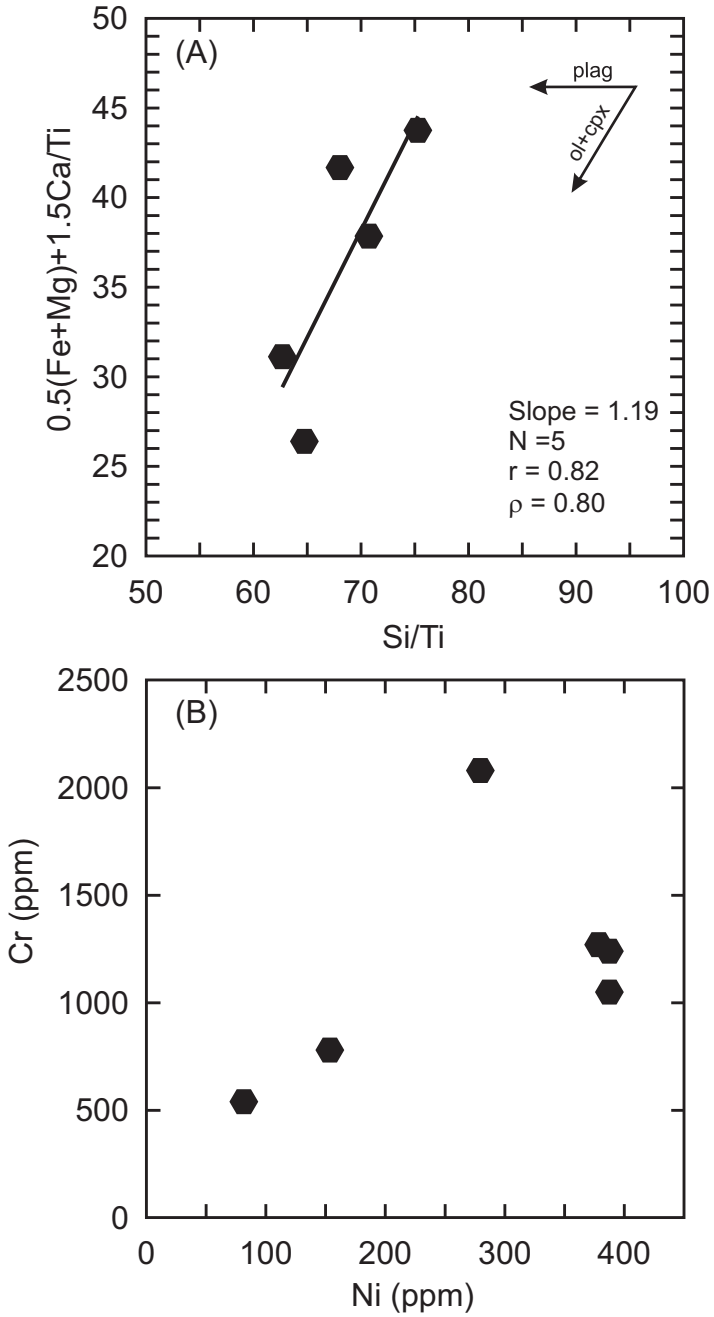

Fig. 8. (A) Pearce element ratio plot of the basaltic rocks from PJ4 showing a trend line indicative of clinopyroxene + olivine fractionation. The correlation coefficient (r) and Spearman rank correlation coefficient (ρ) are both ≥ 0.8. (B) Cr (ppm) vs. Ni (ppm) of the same rocks showing a positive correlation.

melts fractionate clinopyroxene and olivine (fig. 8). Fractionation of silicate minerals in the PJ4 samples and in the high-Ti Pahalgam rocks probably did not have a significant effect on the concentration of heavy rare earth elements (Yb, Lu, Y) or the

light rare earth elements (La, Ce, Nd) because they tend not to partition into those minerals. Therefore most high field strength element ratios (La/Yb_N, Nb/Y, Zr/Y) associated with residual garnet were not affected and thus the partial melt models of a spinel peridotite are likely to be valid. However sample PJ4-004 is different from all other mafic samples as it has very high MgO (~22.1 wt%) content, very low total alkali (Na_2O+K_2O = 0.1 wt%) contents, and has a La/Yb_N ratio of 1.0. The relict rock textures show large (1–3 mm diameter), rounded pseudomorphs of serpentine within a fine grained groundmass. Serpentine likely replaced olivine crystals suggesting the rock is a porphyry and thus not likely to be a melt composition.

The amount of partial melting from the mantle source appears to be the primary influence on the composition of the mafic Panjal Traps. In some cases the basalts have experienced crystal fractionation and show evidence of crustal contamination (figs. 5 and 7D). There are volumetrically minor andesitic rocks at Guryal Ravine and at section PJ4 (PJ4-003). The andesitic rocks of the Panjal Traps are chemically similar as they have high SiO_2 (>54 wt%) contents, enriched $\varepsilon_{Nd}(t)$ ($\varepsilon_{Nd}(t)$ = −6.8 to −6.1) values and intermediate trace element signatures between the Panjal basalts and silicic volcanic rocks. Previous work suggests that the andesitic rocks are derived by mixing between the silicic melts and mafic melts during the earlier stages of volcanism (Shellnutt and others, 2014). The silicic rocks are identified as dacites and rhyolites and have enriched $\varepsilon_{Nd}(t)$ values ($\varepsilon_{Nd}(t)$ = −8.6 to −8.9) that are similar to the $\varepsilon_{Nd}(t)$ values ($\varepsilon_{Nd}(t)$ = −10 to −15) of Himalayan crust (Spencer and others, 1995). The SiO_2 and TiO_2 concentrations are very different (dacites $SiO_2 \approx 65$ wt%, $TiO_2 \approx 1.1$ wt%; rhyolites $SiO_2 \approx 75$ wt%, $TiO_2 \approx 0.4$ wt%) between the dacites and rhyolites and it is uncertain whether just the dacitic melts, just the rhyolitic melts or both mixed with mafic melts to produce the andesites. If a mafic composition equal to PJ4-001 (TiO_2 = 1.1 wt%) mixed with a rhyolitic melt at ~25 percent then the TiO_2 content would decrease and be similar to sample PJ4-003 (TiO_2 = 0.9 wt%) whereas in the case of a dacite melt mixing the TiO_2 would be maintained at ~1.1 weight percent thus mixing of the rhyolitic melt is preferred in the case of the PJ4 andesite however this may not be applicable to all andesitic rocks (for example, PJ1-010 and PJ1-030 in Shellnutt and others, 2014) and in some cases they may represent dacite-basalt hybrids.

The hybrid nature of the andesitic Panjal Traps is strong evidence in support of crustal contamination within some of the basaltic rocks but not all basalts experienced such significant contamination. There is a minority of basalts that do not show evidence for crustal contamination ($Th/Nb_{PM} < 2.5$) and have the least isotopically enriched samples ($\varepsilon_{Nd}(t) > -1.0$) whereas other samples show varying amounts of contamination and isotopic enrichment but less than the andesitic rocks ($Th/Nb_{PM} > 2.5$; $\varepsilon_{Nd}(t) < -1.9$). The amount of crustal contamination was estimated to be < 20 percent for an individual basaltic sample but more commonly between 5 percent and 10 percent in each Ti-group (Shellnutt and others, 2014). Isotope mixing calculations for the PJ4 samples indicate that 5 percent to 10 percent mixing between sample PJ4-007 ($\varepsilon_{Nd}(t)$ = +4.3) and a Panjal rhyolite ($\varepsilon_{Nd}(t)$ = −8.7) will produce the moderately enriched $\varepsilon_{Nd}(t)$ value for samples PJ4-001 ($\varepsilon_{Nd}(t)$ = +0.3). The PJ3 samples have $\varepsilon_{Nd}(t)$ values ($\varepsilon_{Nd}(t)$ = −3.9 to −2.5) similar to the most depleted ($\varepsilon_{Nd}(t)$ = −3.1) low-Ti basalts from Pahalgam thus it is difficult to determine if there was crustal contamination or if the source was initially enriched. If crustal assimilation occurred within the PJ3 samples and assuming the most depleted sample represents the primary composition then no more than 5 percent crustal assimilation would be required to change the $\varepsilon_{Nd}(t)$ value from −2.9 to −3.9.

In summary, the basaltic rocks from PJ3 and PJ4, much like the basalts from Guryal Ravine and Pahalgam, can be modeled by moderate to high amounts (≈5 to ≈15%) of partial melting of a spinel peridotite source. The rocks from PJ4 show

evidence of fractionation of clinopyroxene and olivine whereas the rocks from PJ3 do not show evidence for silicate mineral fractionation. Crustal contamination plays a major role in the genesis of the andesitic rocks (≈25% crustal assimilation) whereas the basaltic rocks may have assimilated ≤ 10 percent crustal material.

Mantle Source Compositions Related to the Transition from Continental Rift to Ocean Basin

The whole rock major and trace elemental and Sr-Nd isotope data indicate that the mafic Panjal Traps from the Kashmir Valley do not represent an eruption of monotonous, chemically similar basalts. Although all of the basalts are mildly alkalic to tholeiitic, they show a significant isotopic diversity. The large range of $\varepsilon_{Nd}(t)$ values ($\varepsilon_{Nd}(t) \approx -5.0$ to $+4.3$) of the basalts suggests that a single mantle source is unlikely. The I_{Sr} values are more difficult to interpret as many samples have very high values ($I_{Sr} > 0.7113$) and the rocks have experienced greenschist facies metamorphic conditions suggesting mobility of Rb or Sr or both. Two samples (PJ4-005 and PJ4-006) from section PJ4 as well as a few others from Guryal Ravine and Pahalgam have I_{Sr} values between 0.7060 and 0.7090 with corresponding $\varepsilon_{Nd}(t)$ values between -2.0 and $+3.4$ (fig. 5). The low $\varepsilon_{Nd}(t)$ values and high $^{87}Sr/^{86}Sr$ isotope ratios are similar to the enriched mantle II (EMII) source composition described by Zindler and Hart (1986), Workman and others (2004) and Workman and Hart (2005) but could be an artifact of crustal assimilation.

The andesitic rocks likely represent the extreme example of magma-crustal melt mixing in the Panjal system but offer insight into the initial mantle source composition. The fact that the andesites have $\varepsilon_{Nd}(t)$ values < -6 suggests that the basalts with moderately isotopically enriched characteristics ($\varepsilon_{Nd}(t) \approx -3.0$ to $+1.0$) could not become enriched solely due to crustal assimilation because the amount of crustal material required to change the isotopic composition from depleted mantle values ($\varepsilon_{Nd}(t) = +10$) to < -6 would exceed reasonable amounts of assimilation (for example, ≈25% assimilation) and thus the rocks would no longer be basaltic. In other words, the moderately enriched basalts were derived from a mantle source that was originally enriched (Shellnutt and others, 2014). In contrast the more depleted Nd-isotope ($\varepsilon_{Nd}(t) \approx +2.4$ to $+4.3$) samples from section PJ4 suggest they are from a more depleted mantle source and experienced a different process of enrichment. The stratigraphic variation of the Nd isotope ratios shows two distinct trends (figs. 9A and 9B). The samples from Guryal Ravine and Pahalgam show similar variation from the basal basalts to the top. In both cases the basal basalts have moderately enriched Nd-isotopes ($\varepsilon_{Nd}(t) \approx +1.0$) followed by enriched ($\varepsilon_{Nd}(t) \approx -4.0$) samples, then less enriched ($\varepsilon_{Nd}(t) \approx -2.0$) samples followed by more enriched samples ($\varepsilon_{Nd}(t) \approx -4.0$). The profile from PJ4 shows a very different pattern (fig. 9C). The bottom sample starts with a moderately enriched sample followed by a highly enriched andesitic sample. At the 200 m interval the Nd isotopes become moderately depleted and continue to become more depleted up-section. Although it is unlikely the sections are correlative, the fact that the PJ4 basalts become significantly more depleted after the andesite whereas at Guryal Ravine the basalts are still enriched suggests either that crustal contamination is more pervasive in the basalts from the eastern side of the Valley or that the mantle source is becoming isotopically depleted.

Figure 10A shows trend lines represented by the basaltic rocks from Guryal Ravine, Pahalgam and PJ4. The samples from PJ3 plot closer to the Pahalgam line and do not show a linear distribution. The Pahalgam and PJ4 lines converge close to the composition of the Panjal rhyolites whereas the Guryal Ravine line passes near the Panjal dacites suggesting the trend lines represent mixing lines. Moreover the trend lines indicate that two isotopically distinct mantle sources produced the Panjal Traps. The intercept $\varepsilon_{Nd}(t)$ values of the trend lines for the Guryal Ravine and Pahalgam samples at the depleted mantle composition ($Th/Nb_{PM} \approx 0.5$) are between -1 and

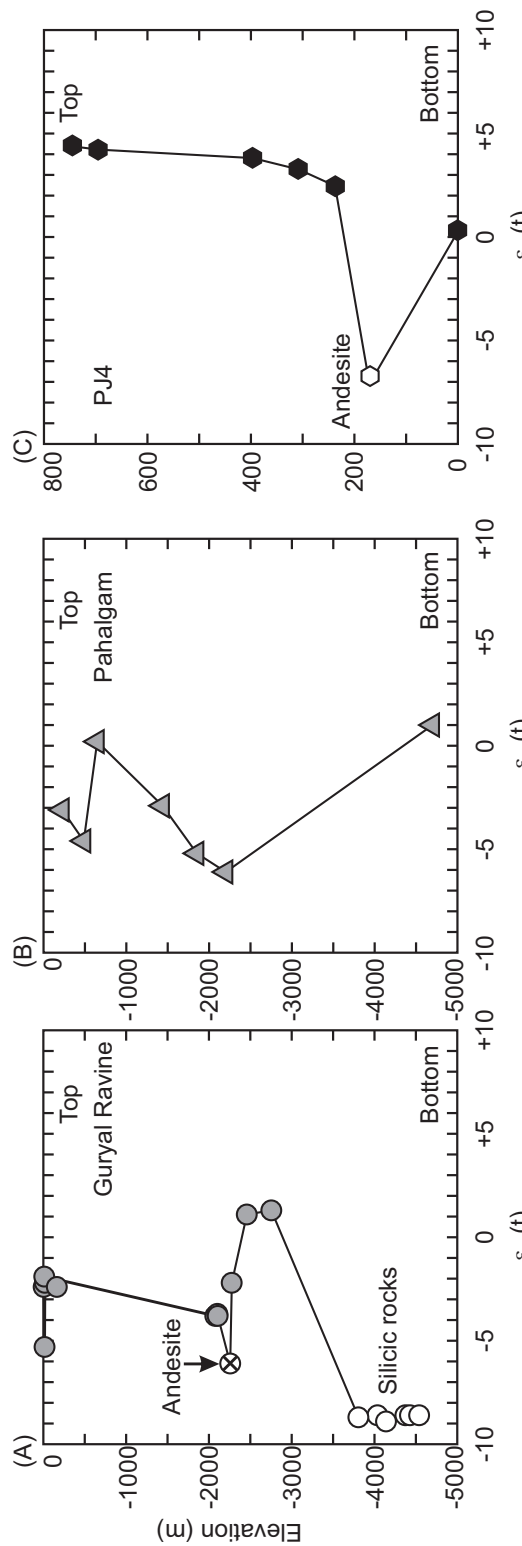

Fig. 9. Chemostratigraphic profiles of Nd-isotopes from (A) Guryal Ravine, (B) Pahalgam and (C) PJ4. The profiles from Guryal Ravine and Pahalgam start at the volcanic-sedimentary contact and moves downward to the final flows. The profile at PJ4 starts at the floor of the Kashmir Valley and moves upward to the summit of the Pir Panjal range.

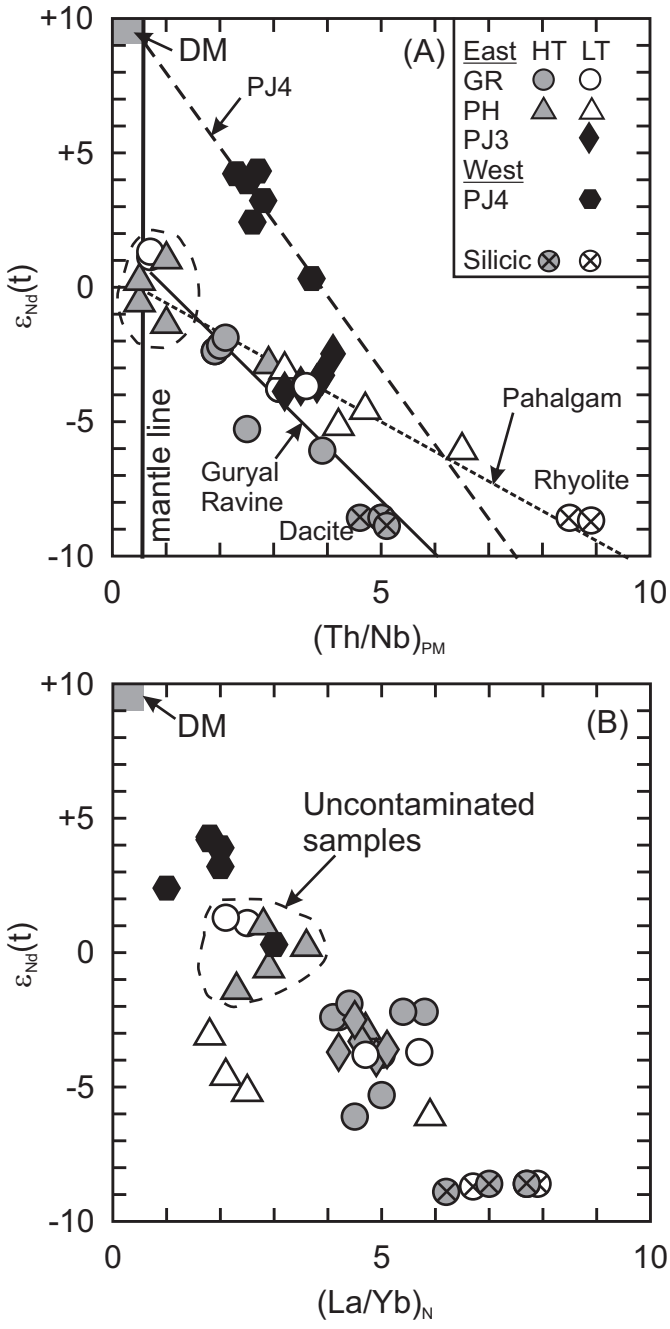

Fig. 10. (A) $\varepsilon_{Nd}(t)$ vs. Th/Nb_{PM} showing three mixing lines of the Panjal basaltic rocks and the Panjal silicic rocks. The mantle line is based on primitive mantle values from Sun and McDonough (1989). The calculated regression lines for the basalt data are extended to the x-axis and the mantle line. (B) $\varepsilon_{Nd}(t)$ vs. La/Yb_N of the Panjal Traps showing the higher $\varepsilon_{Nd}(t)$ and lower La/Yb_N values of the PJ4 samples in comparison with the uncontaminated samples from Guryal Ravine and Pahalgam. DM = depleted mantle values of Workman and Hart (2005).

+1.0 whereas the $\varepsilon_{Nd}(t)$ value for the PJ4 samples is +9. Furthermore figure 10B shows the PJ4 samples plot above and to the left of the 'pristine' mantle source of Guryal Ravine and Pahalgam. The position of the most isotopically depleted PJ4 basalt samples is mostly likely attributed to higher amounts of melting of depleted mantle source that was contaminated by continental crust. Therefore the 'pristine' mantle source of some Guryal Ravine and Pahalgam basaltic rocks is relatively enriched whereas the original source of the PJ4 samples was probably similar to depleted mantle.

The identification of moderately depleted samples suggests that the original magma source could be closer to depleted mantle and that these rocks were derived from an asthenospheric source whereas the enriched melts were derived from a lithospheric mantle source. A two source model would require two separate melting regimes and has been proposed as a possible explanation for some LIPs (Barrat and others, 1993; Sweeney and others, 1994; Pik and others, 1999; Xiao and others, 2004). The two regimes could be facilitated by: 1) an upwelling (mantle plume) of deeper mantle material (sublithospheric mantle) and 2) melting of lithospheric mantle due to lithospheric thinning or heating from a mantle plume or both. The evidence for a mantle plume model is very limited as there is no evidence for structural doming of the crust or definitively correlative ultramafic volcanic rocks but the duration of volcanism appears to be very short as the rocks are constrained to the Sakmarian-Artinskian (Nakazawa and others, 1975; Campbell, 2007). Irrespective of the origin of the Panjal vis-à-vis a mantle plume, a potential problem with the two source model is that there is no evidence for differential source depth. The basaltic rocks can be modeled by partial melting of a spinel peridotite source rather than a garnet peridotite source, additionally the rocks derived by higher amounts of partial melting have more depleted isotopic characteristics and higher Mg# (fig. 11). The Sm/Yb_{PM} values are decreasing with increasing $\varepsilon_{Nd}(t)$ values and Mg# values and indicates that as partial melting increases the more depleted the isotopic values become. The high Mg# samples from Pahalgam and PJ4 are similar to E-MORB which suggests that their source is more depleted and perhaps more isotopically homogeneous. Moreover, at section PJ4 the most isotopically depleted samples are on top of the isotopically enriched rocks (andesite and basalt) suggesting there is a temporal evolution from enriched to depleted compositions. Models such as continuous/dynamic melting could explain the formation of chemically different samples erupting within the same environment but there are numerous factors (for example, variability of partition coefficients, non-cotectic mineral proportions, mineral reactions, differing diffusion times through solid and liquid) which cannot be constrained easily and thus the applicability of this model is uncertain (Langmuir and others, 1977; Shaw, 2000). Additionally, the tectonomagmatic discrimination diagram of Pearce and others (1977) shows the 'low-Ti' rocks from Pahalgam, PJ3 and PJ4 are similar to ocean floor basalts whereas the rocks from Guryal Ravine and high-Ti Pahalgam rocks are similar to continental tholeiites (fig. 12).

It is possible that the explanation for the Nd-isotope and chemical variation lies in the tectonic regime changing from a nascent continental rift to an adolescent rift which is transitioning into a mature ocean basin (Barrat and others, 1993). The initiation of the Panjal continental rift would require a stress field which activated a tensional environment within the southern Tethys margin of Gondwana. The rift would then develop and help create the Cimmerian ribbon-like continent that would eventually accrete to the southern Eurasian margin during the middle Mesozoic closure of the Neo-Tethys Ocean (Metcalfe, 2002, 2006). The chemical evolution of the Panjal basalts from relatively enriched to relatively depleted is probably reflecting the changing nature of the mantle source as the initial mantle melts are likely derived

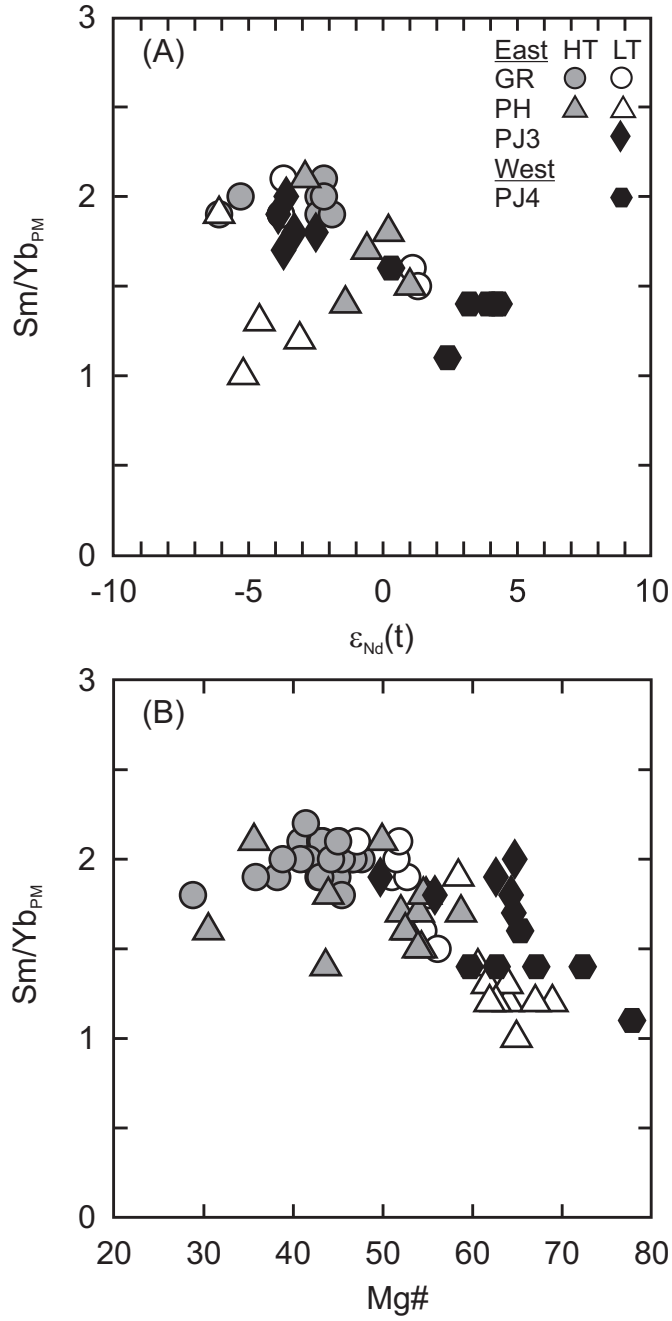

Fig. 11. (A) Sm/Yb_{PM} vs. $\varepsilon_{Nd}(t)$ and (B) Sm/Yb_{PM} vs. Mg# of the mafic Panjal Traps.

from the lithospheric mantle followed by melts which are derived from a source that is becoming more similar to depleted mantle as the rift basin begins to form oceanic crust (fig. 13).

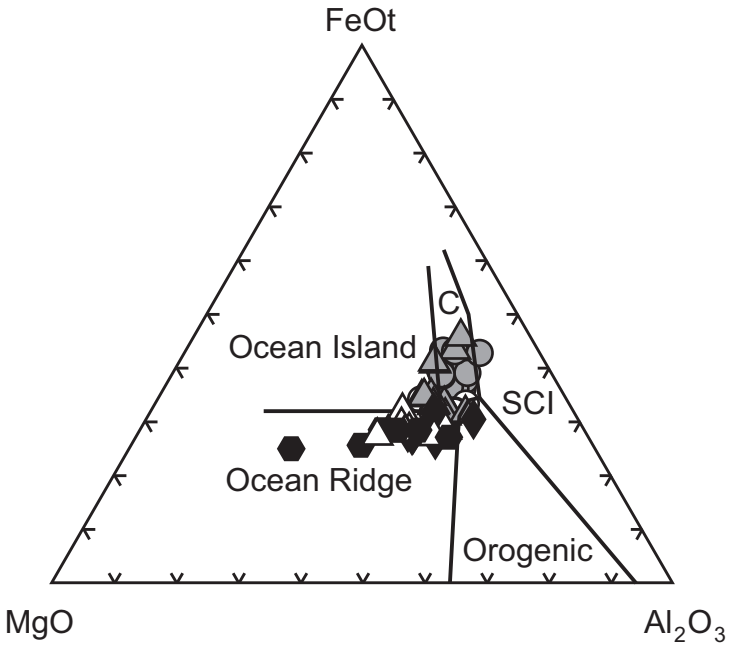

Fig. 12. Basalt tectonomagmatic discrimination diagram of Pearce and others (1977) for the mafic Panjal Traps. C = continental basalts, SCI = spreading center island. Symbols as in figure 2.

Comparison of the Panjal Traps to Pangaean and Post-Pangaean Continental LIPs

The Late Palaeozoic (~300 Ma to ~251 Ma) was a time of substantial continental flood basalt volcanism, the zenith of Pangaea, large polar glaciations and two of seven major mass extinctions occurred (Martin, 1981; Wignall, 2001). The five major continental flood basalt eruptions are: the Skagerrak-Centered large igneous province (~300 Ma), Himalayan event (~290–270 Ma), Tarim large igneous province (~290–270 Ma), Emeishan large igneous province (~260 Ma) and the Siberian Traps (~251 Ma) (Torsvik and others, 2008; Saunders and Reichow, 2009; Zhu and others, 2010; Yang and others, 2013; Shellnutt and others, 2014; Shellnutt, 2014; Wang and others, 2014). The Skagerrak-Centered large igneous province corresponds to volcanic and plutonic rocks within Scandinavia (Oslo graben), Britain (Midland Valley complex and Whin Sill complex) and continental Europe (Torsvik and others, 2008; Timmerman and others, 2009). The Tarim and Emeishan LIPs are constrained geographically to the Tarim and South China Blocks respectively whereas the Siberian Traps are located within the Kuznetsk Basin and Siberian Craton of North-Central Asia. The Himalayan event is an assortment of flood basalts and mafic dikes that are broadly contemporaneous and related to rifting of terranes from the Indian margin of Gondwana of which the most voluminous preserved remnants are the Panjal Traps (Bhat and others, 1981; Bhat, 1984; Zhu and others, 2010; Shellnutt and others, 2011, 2014; Ali and others, 2012; Zhai and others, 2013; Wang and others, 2014).

Upon examination of the average La/Yb ratio normalized to chondritic values (La/Yb_N), Zr/Y ratio, Nb/Y ratio and Nb/La ratio of the Pangaean continental flood basalt provinces of the Late Palaeozoic it is clear that the Panjal Traps have the lowest ratios (table 3; fig. 14). The La/Yb_N, Zr/Y and Nb/Y ratios are indicators of residual garnet in the mantle source from which basaltic melts are derived and thus a proxy for

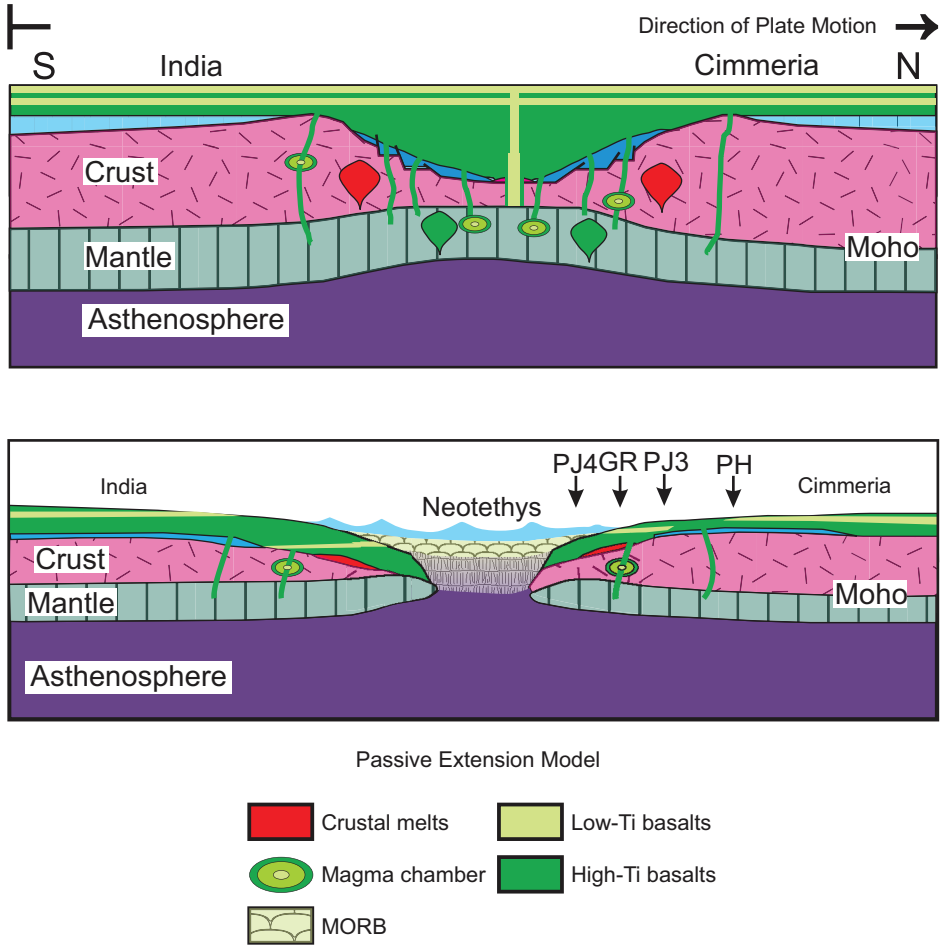

Fig. 13. Tectonic synthesis of the Panjal Traps. (A) The initial subaerial eruption followed by the (B) subaqueous eruptions and eventual opening of the Neotethys Ocean. The relative positioning of the PJ4 (West Kashmir Valley), Guryal Ravine (GR), PJ3 (East Kashmir Valley) and Pahalgam (PH) volcanic profiles for this study.

depth whereas the Nb/La ratio is a measure of crustal influence or contribution from an enriched mantle source (Saunders and others, 1992; Fitton and others, 1997). We do not suggest that the calculated average value of a given LIP implies that all basalts originated from the same mantle source or depth but simply that the prevailing composition of an individual LIP is reflected in the average ratio. The high field strength element ratios of the Tarim Traps, Emeishan Traps and Skagerrak basalts are higher and consistent with a garnet-bearing peridotite source, less influence from an enriched lithospheric component and possibly a mantle plume origin (Neumann other others, 2002; Yang and others, 2013; Shellnutt, 2014). On the other hand, comparing the Panjal Traps to the post-Pangaean (~200 Ma to ~55 Ma) LIPs reveals chemical similarity (fig. 14).

Overall, the LIPs associated with plate separation have lower high field strength element ratios, in particular Nb/La (and higher Th/Nb_{PM}) ratios, than non-break-up-related LIPs thus crustal assimilation or influence of an enriched source component

TABLE 3

Average trace element ratios of some LIPs from 300 Ma to 55 Ma

Sample	Age (Ma)	$\frac{La}{Yb_N}$	2σ	n	Zr/Y	2σ	n	$\frac{Nb}{Y}$	2σ	n	Nb/La	2σ	n	$\frac{Sm}{Yb_{PM}}$	2σ	n	$\frac{Th}{Nb_{PM}}$	2σ	n
NAT	55	3.5	0.4	482	4.0	0.1	710	0.33	0.03	710	0.9	0.0	709	2.1	0.2	447	2.2	0.3	554
Deccan	65	5.3	0.5	437	5.1	0.2	497	0.62	0.06	501	0.9	0.0	502	2.6	0.1	409	2.1	0.2	386
Madagascar	90	4.3	0.5	84	5.2	0.3	173	0.36	0.03	172	0.8	0.1	93	2.5	0.2	85	1.4	0.4	73
Rajmahal	118	5.8	1.5	26	3.6	0.0	49	0.20	0.02	49	0.6	0.1	36	1.7	0.1	26	1.6	0.7	18
Etendeka	132	5.2	0.8	86	4.6	0.3	108	0.48	0.09	108	0.7	0.1	108	2.3	0.2	86	1.8	0.2	87
Parana	132	6.3	0.6	82	5.6	0.3	98	0.52	0.04	98	0.7	0.0	98	2.6	0.2	71	1.8	0.2	80
Karoo	183	5.3	0.3	584	4.4	0.2	624	0.33	0.02	623	0.7	0.0	625	2.1	0.1	534	1.8	0.4	545
CAMP	200	3.2	0.2	494	3.9	0.1	447	0.27	0.01	494	0.7	0.0	494	1.6	0.1	475	2.5	0.1	445
Siberia	251	5.5	0.8	193	5.6	0.7	193	0.68	0.18	193	0.9	0.1	193	2.2	0.2	188	1.4	0.1	175
ELIP	260	8.3	0.5	188	7.0	0.3	188	0.80	0.04	188	0.9	0.0	188	3.4	0.2	188	2.0	0.1	188
Panjal	290	3.9	0.3	66	4.0	0.3	66	0.40	0.04	66	0.8	0.1	66	1.8	0.1	66	2.6	0.3	66
Tarim	290	7.9	0.8	74	7.0	0.5	74	0.83	0.08	74	0.9	0.1	74	3.2	0.3	61	1.1	0.1	66
SCLIP	300	16.4	1.0	84	9.2	0.4	81	1.73	0.12	81	1.1	0.1	82	5.2	0.3	84	0.8	0.1	81

NAT = north Atlantic Tertiary Province, CAMP = central Atlantic magmatic province, ELIP = Emeishan large igneous province, SCLIP = Skagerrak-centered large igneous province. N = normalized to chondrite value of Sun and McDonough (1989). PM = normalized to primitive mantle value of Sun and McDonough (1989). n = number of samples.

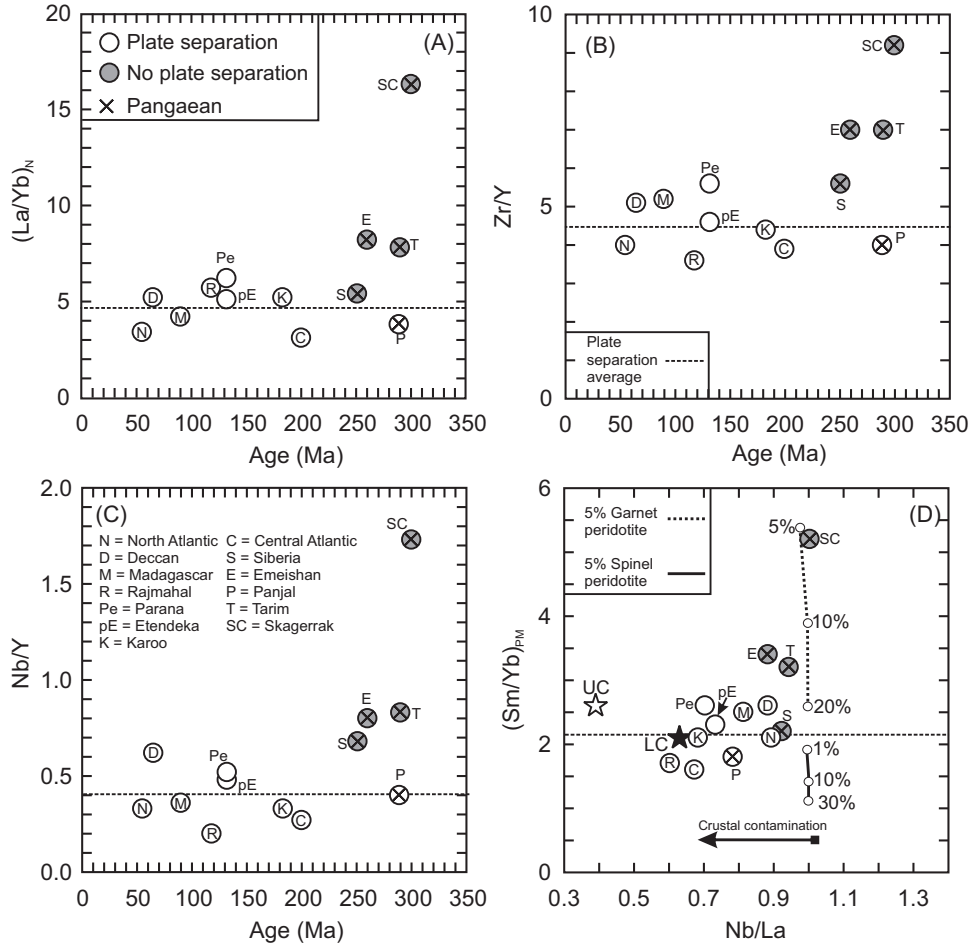

Fig. 14. Temporal variations of (A) La/Yb_N, (B) Zr/Y and (C) Nb/Y and (D) $(Sm/Yb)_{PM}$ vs. Nb/La of Late Carboniferous to Paleogene continental LIPs. The Pangaean LIPs are from 300 Ma to 250 Ma. N= North Atlantic Tertiary Province, D = Deccan Traps, M = Cretaceous igneous province of Madagascar; R = Rajmahal Traps; pE = Etendeka LIP, Pe = Parana LIP, K = Karoo, C = Central Atlantic Magmatic Province, S = Siberian Traps, E = Emeishan LIP, T = Tarim LIP, P = Panjal Traps, SC = Skagerrak-Centered LIP. La/Yb_N denotes normalized to chondrite values of Sun and McDonough (1989). The LIPs were selected on the basis of their age (that is, < 300 Ma) and their unambiguous tectonic setting (plate separation vs. non-plate separation). Some of the LIPs are amongst the largest (Siberian Traps, Deccan Traps, Parana, CAMP) of the Phanerozoic and were emplaced during the existence and final disintegration of Pangaea. Data was compiled primarily from the GEOROC database maintained by the Max Planck Institute für Chemie in Mainz, Germany (georoc.mpch-mainzgwdg.de/georoc/) whereas other supplementary sets (for example, Skagerrak-Centered, Panjal Traps) were collected from different sources (Neumann and others, 2002; Shellnutt and others, 2014). The data were screened on the basis of major element chemistry. Samples geochemically classified as basalt (that is, SiO_2 = 45 to 52 wt.%; $Na_2O+K_2O \leq 5$ wt.%; MgO < 16 wt.%) according to the scheme of LeBas and others (1986) with LOI < 2.5 and a sum total between 98 and 102 wt% (including LOI) were used.

may be more prevalent in the post-Pangaean LIPs and the Panjal Traps. Furthermore the Zr/Y and Sm/Yb_{PM} ratios, which are less sensitive to crustal assimilation, reveal a similar distribution as La/Yb_N and Nb/Y. The process of continental break-up probably enhances crustal assimilation because the basaltic magmas are likely to be in contact with the continental crust for a longer period of time (Fitton and others, 2000;

Rooney and others, 2007). The time between the initial eruption of flood basalts and the formation of oceanic crust can take ~20 million years or more as opposed to eruption durations of ≤ 10 million years for non-plate separation LIPs (Janney and Castillo, 2001; Bryan and Ernst, 2008). Consequently, it seems the Panjal Traps have more in common with the post-Pangaean LIPs that are related to the opening of the Atlantic Ocean (Central Atlantic Magmatic Province, Parana-Etendeka LIP, North Atlantic Igneous Province) and the break-up of Gondwana (Karoo, Rajmahal, Madagascar, Deccan).

Perhaps the most intriguing aspect of the diagrams in figure 14 is that the plate-separation LIPs are relative uniform in their La/Yb_N, Zr/Y and Nb/Zr despite being of various ages and having unique geological conditions, for example the age and composition of the crust that the basaltic magmas passed through. Moreover the Sm/Yb_{PM} ratios reveal there may be at least three different mantle compositions responsible for the basaltic rocks. Partial melt curves of a 5 percent garnet peridotite (55% olivine, 25% orthopyroxene, 15% clinopyroxene) and 5 percent spinel peridotite (55% olivine, 25% orthopyroxene, 15% clinopyroxene) are plotted on figure 14D. The curves highlight the influence garnet has on the Sm/Yb ratio compared to spinel peridotite but it also shows that the Skagerrak, Tarim and Emeishan basalts are more influenced by a garnet peridotite source, whereas the Central Atlantic, Panjal and Rajmahal basalts are more influenced by a spinel peridotite source (~1% to ~10%). The basalts from the remaining LIPs fall between the end-member partial melt curves suggesting they may be derived from a source that contains variable quantities of both spinel and garnet. Thus it is possible that the basalts of the Skagerrak, Tarim and Emeishan LIPs are derived from a deep source, the basalts of the Central Atlantic, Panjal and Rajmahal LIPs are derived from a shallow source and the remaining LIPs are derived by melting at or near the garnet/spinel transition zone.

CONCLUSIONS

The mafic Panjal Traps collected from locations at PJ3 and PJ4 show distinct chemical differences and suggest that two mantle sources are required to explain their origin. The basaltic rocks from PJ3 are compositionally similar to the low-Ti basalts from the Pahalgam area and are likely derived by partial melting of a spinel-bearing subcontinental lithospheric mantle source. Trace element ratios (Th/Nb_{PM}) and Nd-isotope mixing modeling indicate that the PJ3 samples experienced ≤ 5 percent crustal contamination. In comparison, the basaltic rocks from section PJ4 have the highest Mg# values amongst the Panjal Traps and show the most depleted Nd-isotope signatures. Trace element modeling suggests that they are derived by ≥ 10 percent partial melting of a spinel peridotite source and likely experienced fractionation of clinopyroxene and olivine and ≤ 10 percent crustal contamination. The shift from enriched isotopic signatures to more depleted signatures in the basalts may be owing to melting from an initial lithospheric mantle source during nascent continental rifting to one that is becoming more depleted as a result of ocean basin formation and melting of asthenospheric mantle.

ACKNOWLEDGMENTS

We thank Andy Saunders and Godfrey Fitton for constructive reviews. The authors are very appreciative of the field and laboratory assistance of Ghulam-ud-Din Bhat, G.M. Zaki, Sun-Lin Chung, Fu Long Wang, Carol Chuang, Cynthia Tsai and Emily Lin. This project was supported by NSC grant 102-2628-M-003-001-MY4 to JGS.

REFERENCES

Ali, J. R., Aitchison, J. C., Chik, S. Y. S., Baxter, A. T., and Bryan, S. E., 2012, Paleomagnetic data support Early Permian age for the Arbor volcanics in the lower Siang Valley, NE India: Significance for Gondwana

break-up models: Journal of Asian Earth Sciences, v. 50, p. 105–115, http://dx.doi.org/10.1016/j.jseaes.2012.01.007
Arth, J. G., 1976, Behaviour of trace elements during magmatic processes-a summary of theoretical models and their applications: Journal of Research U.S. Geological Survey, v. 4, p. 41–47.
Baksi, A. K., 2001, Search for a deep-mantle component in mafic lavas using a Nb-Y-Zr plot: Canadian Journal of Earth Sciences, v. 38, n. 5, p. 813–824, http://dx.doi.org/10.1139/cjes-38-5-813
Barrat, J. A., Jahn, B. M., Fourcade, S., and Joron, J. L., 1993, Magma genesis in an ongoing rifting zone: The Tadjoura Gulf (Afar area): Geochimica et Cosmochimica Acta, v. 57, n. 10, p. 2291–2302, http://dx.doi.org/10.1016/0016-7037(93)90570-M
Beattie, P., 1994, Systematics and energetics of trace-element partitioning between olivine and silicate melts: Implications for the nature of mineral/melt partitioning: Chemical Geology, v. 117, n. 1–4, p. 57–71, http://dx.doi.org/10.1016/0009-2541(94)90121-X
Bhat, M. I., 1984, Abor Volcanics: further evidence for the birth of the Tethys Ocean in the Himalayan segment: Journal of the Geological Society, London, v. 141, n. 4, p. 763–775, http://dx.doi.org/10.1144/gsjgs.141.4.0763
Bhat, M. I., and Zainuddin, S. M., 1979, Origin and evolution of the Panjal Volcanics: Himalayan Geology, v. 9, n. 2, p. 421–461.
Bhat, M. I., Zainuddin, S. M., and Rais, A., 1981, Panjal Trap chemistry and the birth of Tethys: Geological Magazine, v. 118, n. 4, p. 367–375, http://dx.doi.org/10.1017/S0016756800032234
Brookfield, M. E., Algeo, T. J., Hannigan, R., Williams, J., and Bhat, G. M., 2013, Shaken *and* stirred: Seismites and tsunamites at the Permian-Triassic boundary, Guryal Ravine, Kashmir, India: Palaios, v. 28, n. 8, p. 568–582, http://dx.doi.org/10.2110/palo.2012.p12-070r
Bryan, S. E., and Ernst, R. E., 2008, Revised definition of large igneous provinces (LIPs): Earth Science-Reviews, v. 86, n. 1–4, p. 175–202, http://dx.doi.org/10.1016/j.earscirev.2007.08.008
Bryan, S. E., and Ferrari, L., 2013, Large igneous provinces and silicic large igneous provinces: Progress in our understanding over the last 25 years: Geological Society of America Bulletin, v. 125, p. 1053–1078, http://dx.doi.org/10.1130/B30820.1
Campbell, I. H., 2007, Testing the plume theory: Chemical Geology, v. 241, n. 3–4, p. 153–176, http://dx.doi.org/10.1016/j.chemgeo.2007.01.024
Chaudhry, M. N., and Ashraf, M., 1980, The volcanic rocks of Poonch District, Azad Kashmir: Proceedings of the International Committee of Geodynamics Group 6, Kashmir Special issue, Geological Bulletin of the University of Peshawar, v. 13, p. 121–128.
Chauvet, F., Lapierre, K., Bosch, D., Guillot, S., Mascle, G., Vannay, J.-C., Cotten, J., Brunet, P., and Keller, F., 2008, Geochemistry of the Panjal Traps basalts (NW Himalaya): records of the Pangea Permian break-up: Bulletin de la Société Géologique de France, v. 179, n. 4, p. 383–395, http://dx.doi.org/10.2113/gssgfbull.179.4.383
Coffin, M. F., and Eldholm, O., 1994, Large igneous provinces: Crustal structure, dimensions and external consequences: Reviews in Geophysics, v. 32, n. 1, p. 1–36, http://dx.doi.org/10.1029/93RG02508
Courtillot, V. E., and Renne, P. R., 2003, On the ages of flood basalt events: Comptes Rendus Geoscience, v. 335, n. 1, p. 113–140, http://dx.doi.org/10.1016/S1631-0713(03)00006-3
Courtillot, V., Jaupart, C., Manighetti, I., Tapponier, P., and Besse, J., 1999, On the causal links between flood basalts and continental break-up: Earth and Planetary Science Letters, v. 166, n. 3–4, p. 177–195, http://dx.doi.org/10.1016/S0012-821X(98)00282-9
Ernst, R. E., and Buchan, K. L., 2001, Large mafic magmatic events through time and links to mantle plume-heads, *in* Ernst, R. E., and Buchan, K. L., editors, Mantle Plumes: Their Identification Through Time: Geological Society of America Special Papers, v. 352, p. 483–57, http://dx.doi.org/10.1130/0-8137-2352-3.483
Ernst, R. E., Buchan, K. L., and Campbell, I. H., 2005, Frontiers in large igneous province research: Lithos, v. 79, n. 3–4, p. 271–297, http://dx.doi.org/10.1016/j.lithos.2004.09.004
Fitton, J. G., Saunders, A. D., Norry, M. J., Hardarson, B. S., and Taylor, R. N., 1997, Thermal and chemical structure of the Iceland plume: Earth and Planetary Science Letters, v. 153, n. 3–4, p. 197–208, http://dx.doi.org/10.1016/S0012-821X(97)00170-2
Fitton, J. G., Larsen, L. M., Saunders, A. D., Hardarson, B. S., and Kempton, P. D., 2000, Paleogene continental to oceanic magmatism on the SE Greenland continental margin at 63°N: a review of the results of ocean drilling programs legs 152 and 163: Journal of Petrology, v. 41, n. 7, p. 951–966, http://dx.doi.org/10.1093/petrology/41.7.951
Foulger, G. R., 2010, Plates vs. Plumes: A Geological Controversy: Chicester, West Sussex, Wiley-Blackwell, 328 p.
Fuchs, G., 1987, The geology of southern Zanskar (Ladakh) –E vidence for the autochthony of the Tethys Zone of the Himalaya: Jahrbuch der Geologischen Bundesanstal, v. 130, p. 465–491.
Fujimaki, H., Tatsumoto, M., and Aoki, K.-i., 1984, Partition coefficients of Hf, Zr, and REE between phenocrysts and groundmasses: Journal of Geophysical Research-Solid Earth, v. 89, n. 502, p. B662–B672, http://dx.doi.org/10.1029/JB089iS02p0B662
Gaetani, M., Casnedi, R., Fois, E., Gazanti, E., Jadoul, F., Nicora, A., and Tintori, A., 1986, Stratigraphy on the Tethys Himalaya in Zanskar, Ladakh: Rivisita Italiana di Paleontologia e Stratigrafia, v. 91, n. 4, p. 443–478.
Ganju, P. N., 1944, The Panjal Traps: Acid and basic volcanic rocks: Proceedings of the Indian Academy of Sciences, v. 18, p. 125–131.
Garzanti, E., Nicora, A., and Tintori, A., 1992, Late Paleozoic to Early Mesozoic stratigraphy and sedimentary evolution of central Dolpo (Nepal Himalaya): Rivisita Italiana di Paleontologia e Stratigrafia, v. 98, n. 3, p. 271–298.
Garzanti, E., Nicora, A., Tintori, T., Sciunnach, D., and Angiolini, L., 1994, Late Paleozoic stratigraphy and

petrography of the Thini Chu Group (Manang, Central Nepal): Sedimentary record of Gondwana glaciation and rifting of Neotethys: Rivisita Italiana di Paleontologia e Stratigrafia, v. 100, n. 2, p. 155–194.

Garzanti, E., Angiolini, L., and Sciunnach, D., 1996a, The mid-Carboniferous to lowermost Permian succession of Spiti (Po Group and Ganmachidam Formations; Tethys Himalaya, northern India): Gondwana glaciation and rifting of Neo-Tethys: Geodinamica Acta, v. 9, n. 2–3, p. 78–100, http://dx.doi.org/10.1080/09853111.1996.11105279

_____ 1996b, The Permian Kulung Group (Spiti, Lahaul and Zanskar; NW Himalaya): sedimentary evolution during rift/drift transition and initial opening of Neo-Tethys: Rivisita Italiana di Paleontologia e Stratigrafia, v. 102, p. 175–200.

Garzanti, E., Angiolini, L., Brunton, H., Sciunnach, D., and Balini, M., 1998, The Bashkirian "Fenestella Shales" and the Moscovian "Chaetetid Shales" of the Tethys Himalaya (South Tibet, Nepal and India): Journal of Asian Earth Sciences, v. 16, n. 2–3, p. 119–141, http://dx.doi.org/10.1016/S0743-9547(98)00006-3

Garzanti, E., Le Fort, P., and Sciunnach, D., 1999, First report of Lower Permian basalts in south Tibet: tholeiitic magmatism during break-up and incipient opening of Neotethys: Journal of Asian Earth Sciences, v. 17, n. 4, p. 533–546, http://dx.doi.org/10.1016/S1367-9120(99)00008-5

Green, T. H., Sie, S. H., Ryan, C. G., and Cousens, D. R., 1989, Proton microprobe-determined partitioning of Nb, Ta, Zr, Sr and Y between garnet, clinopyroxene and basaltic magma at high pressure and temperature: Chemical Geology, v. 74, n. 3–4, p. 201–216, http://dx.doi.org/10.1016/0009-2541(89)90032-6

Green, T. H., Blundy, J. D., Adam, J., and Yaxley, G. M., 2000, SIMS detemination of trace element partition coefficients between garnet, clinopyroxene and hydrous basaltic liquids at 2-7.5 Gpa and 1080-1200°C: Lithos, v. 53, n. 3–4, p. 165–187, http://dx.doi.org/10.1016/S0024-4937(00)00023-2

Irving, A. J., and Frey, F. A., 1978, Distribution of trace elements between garnet megacrysts and host volcanic liquids of kimberlitic to rhyolitic composition: Geochimica et Cosmochimica Acta, v. 42, n. 6, p. 771–787, http://dx.doi.org/10.1016/0016-7037(78)90092-3

Janney, P. E., and Castillo, P. R., 2001, Geochemistry of the oldest Atlantic oceanic crust suggests mantle plume involvement in the early history of the central Atlantic Ocean: Earth and Planetary Science Letters, v. 192, n. 3, p. 291–302, http://dx.doi.org/10.1016/S0012-821X(01)00452-6

Jenner, G. A., Foley, S. F., Jackson, S. E., Green, T. H., Fryer, B. J., and Longerich, H. P., 1994, Determination of partition coefficients for trace elements in high pressure-temperature experimental run products by laser ablation microprobe-inductively coupled plasma-mass spectrometry (LAM-ICP-MS): Geochimica et Cosmochimica Acta, v. 57, n. 23–24, p. 5099–5103, http://dx.doi.org/10.1016/0016-7037(93)90611-Y

Jerram, D. A., and Widdowson, M., 2005, The anatomy of continental flood basalt provinces: geological constraints on the processes and products of flood volcanism: Lithos, v. 79, n. 3–4, p. 385–405, http://dx.doi.org/10.1016/j.lithos.2004.09.009

Johnson, K. T. M., 1994, Experimental cpx/ and garnet/melt partitioning of *REE* and other trace elements at high pressures: Petrogenetic implications: Mineralogical Magazine, v. 58A, p. 454–455.

Klemme, S., Gunther, D., Hametner, K., Prowatke, S., and Zack, T., 2006, The partitioning of trace elements between ilmenite, ulvospinel, armalcolite and silicate melts with implications for the early differentiation of the moon: Chemical Geology, v. 234, n. 3–4, p. 251–263, http://dx.doi.org/10.1016/j.chemgeo.2006.05.005

Langmuir, C. H., Bender, J. F., Bence, A. E., Hanson, G. N., and Taylor, S. R., 1977, Petrogenesis of basalts from the FAMOUS area: Mid-Atlantic Ridge: Earth and Planetary Science Letters, v. 36, n. 1, p. 133–156, http://dx.doi.org/10.1016/0012-821X(77)90194-7

LeBas, M. J., LeMaitre, R. W., Streckeisen, A., and Zanettin, B., 1986, A chemical classification of volcanic rocks based on the total alkali silica diagram: Journal of Petrology, v. 27, n. 3, p. 745–750, http://dx.doi.org/10.1093/petrology/27.3.745

Lightfoot, P. C., Hawkesworth, C. J., Hergt, J., Naldrett, A. J., Gorbachev, N. S., Fedorenko, V. A., and Doherty, W., 1993, Remobilisation of the continental lithosphere by a mantle plume: major-, trace-element, and Sr-, Nd-, and Pb-isotope evidence from picritic and tholeiitic lavas of the Noril'sk district, Siberian Trap, Russia: Contributions to Mineralogy and Petrology, v. 114, n. 2, p. 171–188, http://dx.doi.org/10.1007/BF00307754

Lydekker, R., 1883, Geology of Kashmir and Chamba territories and the British district of Khagan: Memoirs of the Geological Society of India, v. 22, p. 211–224.

Martin, H., 1981, The late Paleozoic Gondwana glaciation: Geologische Rundschau, v. 70, n. 2, p. 480–496, http://dx.doi.org/10.1007/BF01822128

McKenzie, D., and O'Nions, R. K., 1991, Partial melt distributions from inversion of Rare Earth Element concentrations: Journal of Petrology, v. 32, n. 5, p. 1021–1091, http://dx.doi.org/10.1093/petrology/32.5.1021

Metcalfe, I., 2002, Permian tectonic framework and palaeogeography of SE: Journal of Asian Earth Sciences, v. 20, n. 6, p. 551–566, http://dx.doi.org/10.1016/S1367-9120(02)00022-6

_____ Paleozoic and Mesozoic tectonic evolution and palaeogeography of East Asian crustal fragment: the Korean peninsula in context: Gondwana Research, v. 9, n. 1–2, p. 24–46, http://dx.doi.org/10.1016/j.gr.2005.04.002

Middlemiss, C. S., 1910, Revision of the Silurian-Trias Sequence in Kashmir: Records of the Geological Survey of India, v. 40, p. 206–260.

Myrow, P. M., Snell, K. E., Hughes, N. C., Paulsen, T. S., Heim, N. A., and Parcha, S. K., 2006, Cambrian depositional history of the Zanskar Valley region of the Indian Himalaya: tectonic implications: Journal of Sedimentary Research, v. 76, n. 2, p. 364–381, http://dx.doi.org/10.2110/jsr.2006.020

Nakazawa, K., and Kapoor, H. M., 1973, Spilitic pillow lava in Panjal Trap of Kashmir, India: Memoirs of the Faculty of Science, Kyoto University, Series of Geology and Mineralogy, v. 39, p. 83–98.

Nakazawa, K., Kapoor, H. M., Ishii, K.-I., Bando, Y., Okimura, Y., Tokuoka, T., Murata, M., Nakamura, K., Nogami, Sakagami, S., and Shimizu, D., 1975, The upper Permian and the lower Triassic in Kashmir, India: Memoirs of the Faculty of Science, Kyoto University, Series of Geology and Mineralogy, v. 42, p. 1–106.

Neumann, E.-R., Dunworth, E. A., Sundvoll, B. A., and Tollefsrud, J. I., 2002, B_1 basaltic lavas in Vestfold-Jeløya area, central Oslo rift: derivation from initial melts formed by progressive partial melting of an enriched mantle source: Lithos, v. 61, n. 1–2, p. 21–53, http://dx.doi.org/10.1016/S0024-4937(02)00068-3

Papritz, K., and Rey, R., 1989, Evidence for the occurrence of Permian Panjal trap basalts in the Lesser- and Higher-Himalayas of the western syntaxis area, NE Pakistan: Eclogae Geologicae Helvetiae, v. 82, p. 603–627.

Pareek, H. S., 1976, On studies of the agglomerate slate and Panjal Trap in the Jhelum, Liddar, and Sind Valleys, Kashmir: Recordings of the Geological Survey of India, v. 107, p. 12–37.

Pearce, T. H., Gorman, B. E., and Birkett, T. C., 1977, The relationship between major element chemistry and tectonic environment of basic and intermediate volcanic rocks: Earth and Planetary Science Letters, v. 36, n. 1, p. 121–132, http://dx.doi.org/10.1016/0012-821X(77)90193-5

Peate, D. W., 1997, The Parana-Etendeka province, *in* Mahoney, J. J., and Coffin, M. E., editors, Large Igneous Provinces: Continental, Oceanic, and Planetary Flood Volcanism: Geophysical Monograph 100, p. 217–245, http://dx.doi.org/10.1029/GM100p0217

Pik, R., Deniel, C., Coulon, C., Yirgu, G., and Marty, B., 1999, Isotopic and trace element signatures of Ethiopian flood basalts: evidence for plume-lithosphere interactions: Geochimica et Cosmochimica Acta, v. 63, n. 15, p. 2263–2279, http://dx.doi.org/10.1016/S0016-7037(99)00141-6

Rampino, M. R., and Stothers, R. B., 1988, Flood basalt volcanism during the past 250 million years: Science, v. 241, n. 4866, p. 663–668, http://dx.doi.org/10.1126/science.241.4866.663

Rao, D. R., and Rai, H., 2007, Permian komatiites and associated basalts from the marine sediments of Chhongtash Formation, southeast Karakoram, Ladakh, India: Mineralogy and Petrology, v. 91, n. 3–4, p. 171–189, http://dx.doi.org/10.1007/s00710-007-0206-4

Rooney, T., Furman, T., Bastow, I., Ayalew, D., and Yirgu, G., 2007, Lithospheric modification during crustal extension in the Main Ethiopian Rift: Journal of Geophysical Research-Solid Earth, v. 112, B10201, http://dx.doi.org/10.1029/2006JB004916

Salters, V., and Longhi, J., 1999, Trace element partitioning during the initial stages of melting beneath mid-ocean ridges: Earth and Planetary Science Letters, v. 166, n. 1–2, p. 15–30, http://dx.doi.org/10.1016/S0012-821X(98)00271-4

Saunders, A. D., 2005, Large igneous provinces: Origin and environmental consequences: Elements, v. 1, n. 5, p. 259–263, http://dx.doi.org/10.2113/gselements.1.5.259

Saunders, A. D., and Reichow, M., 2009, The Siberian Traps and the end-Permian mass extinction: a critical review: Chinese Science Bulletin, v. 54, n. 1, p. 20–37, http://dx.doi.org/10.1007/s11434-008-0543-7

Saunders, A. D., Storey, M., Kent, R. W., and Norry, M. J., 1992, Consequences of plume-lithosphere interactions, *in* Storey, B. C., Alabaster, T., and Pankhurst, R. J., editors, Magmatism and the Causes of Continental Break-up: Geological Society, London, Special Publications, v. 68, p. 41–60, http://dx.doi.org/10.1144/GSL.SP.1992.068.01.04

Saunders, A. D., England, R. W., Reichow, M. K., and White, R. V., 2005, A mantle plume origin for the Siberian traps: uplift and extension in the west Siberian basin, Russia: Lithos v. 79, n. 3–4, p. 407–424, http://dx.doi.org/10.1016/j.lithos.2004.09.010

Saunders, A. D., Jones, S. M., Morgan, L. A., Pierce, K. L., Widdowson, M., and Xu, Y. G., 2007, Regional uplift associated with continental large igneous provinces: the roles of mantle plumes and the lithosphere: Chemical Geology, v. 241, n. 3–4, p. 282–318, http://dx.doi.org/10.1016/j.chemgeo.2007.01.017

Sengor, A. M. C., 1984, The Cimmeride orogenic system and the tectonics of Eurasia: Geological Society of America Special Papers, v. 195, 82 p, http://dx.doi.org/10.1130/SPE195-p1

_____ 1987, Tectonics of the Tethysides: orogenic collage development in a collisional setting: Annual Review of Earth and Planetary Sciences, v. 15, p. 213–244, http://dx.doi.org/10.1146/annurev.ea.15.050187.001241

Shaw, D. M., 2000, Continuous (dynamic) melting theory revisited: Canadian Mineralogist, v. 38, v. 1041–1063, http://rruff.info/doclib/cm/vol38/CM38_1041.pdf

Shellnutt, J. G., 2014, The Emeishan large igneous province: A synthesis: Geoscience Frontiers, v. 5, n. 3, p. 369–394, http://dx.doi.org/10.1016/j.gsf.2013.07.003

Shellnutt, J. G., Bhat, G. M., Brookfield, M. E., and Jahn, B.-M., 2011, No link between the Panjal Traps (Kashmir) and the Late Permian mass extinctions: Geophysical Research Letters-Solid Earth, v. 38, L19308, http://dx.doi.org/10.1029/2011GL049032

Shellnutt, J. G., Bhat, G. M., Wang, K.-L., Brookfield, M. E., Dostal, J., and Jahn, B.-M., 2012, Origin of the silicic volcanic rocks of the Early Permian Panjal Traps, Kashmir, India: Chemical Geology, v. 334, p. 154–170, http://dx.doi.org/10.1016/j.chemgeo.2012.10.022

Shellnutt, J. G., Bhat, G. M., Wang, K.-L., Brookfield, M. E., Jahn, B.-M., and Dostal, J., 2014, Petrogenesis of the flood basalts from the Early Permian Panjal Traps, Kashmir, India: Geochemical evidence for shallow melting of the mantle: Lithos, v. 204, p. 159–171, http://dx.doi.org/10.1016/j.lithos.2014.01.008

Spencer, D. A., Tonarini, S., and Pognante, U., 1995, Geochemical and Sr-Nd isotopic characterisation of Higher Himalayan ecologites (and associated metabasites): European Journal of Mineralogy, v. 7, n. 1, p. 89–102, http://dx.doi.org/10.1127/ejm/7/1/0089

Stothers, R. B., 1993, Flood basalts and extinction events: Geophysical Research Letters, v. 20, n. 13, p. 1399–1402, http://dx.doi.org/10.1029/93GL01381
Sun, S.-s., and McDonough, W. F., 1989, Chemical and isotopic systematics of oceanic basalts: implications for mantle composition and processes, *in* Saunders, A. D., and Norry, M. J., editors, Magmatism in the Ocean Basins: Geological Society, London, Special Publications, v. 42, p. 313–435, http://dx.doi.org/10.1144/GSL.SP.1989.042.01.19
Sweeney, R. J., Duncan, A. R., and Erlank, A. J., 1994, Geochemistry and Petrogenesis of central Lebombo basalts of the Karoo igneous province: Journal of Petrology, v. 35, n. 1, p. 95–125, http://dx.doi.org/10.1093/petrology/35.1.95
Timmerman, M. J., Heeremans, M., Kirstein, L. A., Larsen, B. T., Spencer-Dunworth, E.-A., and Sundvoll, B., 2009, Linking changes in tectonic style with magmatism in northern Europe during the late Carboniferous to latest Permian: Tectonophysics, v. 473, n. 3–4, p. 375–390, http://dx.doi.org/10.1016/j.tecto.2009.03.011
Torsvik, T. H., Smethurst, M. A., Burke, K., and Steinberger, B., 2008, Long term stability in deep mantle structure: evidence from the ~300 Ma Skagerrak-Centered large igneous province (the SCLIP): Earth and Planetary Science Letters, v. 267, n. 3–4, p. 444–452, http://dx.doi.org/10.1016/j.epsl.2007.12.004
Torsvik, T. H., van der Voo, R., Doubrovine, P. V., Burke, K., Steinberger, B., Ashwal, L. D., Trønnes, R. G., Webb, S. J., and Bull, A., 2014, Deep mantle structure as a reference frame for movements in and on the Earth: Proceedings of the National Academy of Science, v. 111, n. 24, p. 8735–8740, http://dx.doi.org/10.1073/pnas.1318135111
Vannay, J. C., and Spring, L., 1993, Geochemistry of the continental basalts within the Tethyan Himalaya of Lahul-Spiti and SE Zanzkar (NW India), *in* Trelor, P. J., and Searle, M., editors, Himalayan Tectonics: Geological Society, London, Special Publications, v. 74, p. 237–249, http://dx.doi.org/10.1144/GSL.SP.1993.074.01.17
Wadia, D. N., 1934, The Cambrian-Trias sequence of North-Western Kashmir (Parts of Muzaffarabad and Baramular districts): Records of the Geological Survey of India, v. 68, p. 121–176.
_____1961, Geology of India: London, McMillan and Company, 536 p.
Wang, M., Li, C., Wu, Y.-W., and Xie, C.-M., 2014, Geochronology, geochemistry, Hf isotopic compositions and formation mechanism of radial mafic dikes in northern Tibet: International Geology Review, v. 56, n. 2, p. 187–205, http://dx.doi.org/10.1080/00206814.2013.825076
Wignall, P. B., 2001, Large igneous provinces and mass extinctions: Earth Science Reviews, v. 53, n. 1–2, p. 1–33, http://dx.doi.org/10.1016/S0012-8252(00)00037-4
Winchester, J. A., and Floyd, P. A., 1977, Geochemical discrimination of different magma series and their differentiation products using immobile elements: Chemical Geology, v. 20, p. 325–343, http://dx.doi.org/10.1016/0009-2541(77)90057-2
Workman, R. K., and Hart, S. R., 2005, Major and trace element composition of the depleted MORB mantle (DMM): Earth and Planetary Science Letters, v. 231, n. 1–2, p. 53–72, http://dx.doi.org/10.1016/j.epsl.2004.12.005
Workman, R. K., Hart, S. R., Jackson, M., Regelous, M., Farley, K. A., Blusztajn, J., Kurz, M., and Staudigel, H., 2004, Recycled metasomatized lithosphere as the origin of the Enriched Mantle II (EM2) end-member: Evidence from the Samoan volcanic chain: Geochemistry, Geophysics, Geosystems, v. 5, n. 4, Q04008, http://dx.doi.org/10.1029/2003GC000623
Xiao, L., Xu, Y. G., Mei, H. J., Zheng, Y. F., He, B., and Pirajno, F., 2004, Distinct mantle sources of low-Ti and high-Ti basalts from the western Emeishan large igneous province, SW China: Implications for plume–lithosphere interaction: Earth and Planetary Science Letters, v. 228, p. 525–546, http://dx.doi.org/10.1016/j.epsl.2004.10.002
Xu, Y., Chung, S.-L., Jahn, B.-M., and Wu, G., 2001, Petrologic and geochemical constraints on the petrogenesis of Permian-Triassic Emeishan flood basalts in southwestern China: Lithos, v. 58, n. 3–4, p. 145–168, http://dx.doi.org/10.1016/S0024-4937(01)00055-X
Yang, S., Chen, H., Li, Z., Li, Y., Yu, X., Li, D., and Meng, L., 2013, Early Permian Tarim large igneous province in northwest China: Science in China, v. 56, n. 12, p. 2015–2026, http://dx.doi.org/10.1007/s11430-013-4653-y
Zhai, Q.-G., Jahn, B.-M., Su, L., Ernst, R. E., Wang, K.-L., Zhang, R.-Y., Wang, J., and Tang, S., 2013, SHRIMP zircon U-Pb geochronology, geochemistry and Sr-Nd-Hf isotopic compositions of a mafic dyke swarm in the Qiangtang terrane, northern Tibet and geodynamic implications: Lithos, v. 174, p. 28–43, http://dx.doi.org/10.1016/j.lithos.2012.10.018
Zhang, C.-L., Li, Z.-X., Li, X.-H., Xu, Y.-G., Zhou, G., and Ye, H.-M., 2010, A Permian large igneous province in Tarim and Central Asian orogenic belt, NW China: Results of a *ca.* 275 Ma mantle plume?: Geological Society of America Bulletin, v. 122, n. 11–12, p. 2020–2040, http://dx.doi.org/10.1130/B30007.1
Zhu, D.-C., Mo, X.-X., Zhao, Z.-D., Niu, Y., Wang, L.-Q., Chu, Q.-H., Pan, G.-T., Xu, J.-F., and Zhou, C.-Y., 2010, Presence of Permian extension- and arc-type magmatism in southern Tibet: paleogeographic implications: Geological Society of America Bulletin, v. 122, n. 7–8, p. 979–993, http://dx.doi.org/10.1130/B30062.1
Ziegler, P. A., and Cloetingh, S., 2004, Dynamic processes controlling evolution of rifted basins: Earth-Science Reviews, v. 64, n. 1–2, p. 1–50, http://dx.doi.org/10.1016/S0012-8252(03)00041-2
Zindler, A., and Hart, S. R., 1986, Chemical geodynamics: Annual Review of Earth and Planetary Sciences, v. 14, p. 493–571, http://dx.doi.org/10.1146/annurev.ea.14.050186.002425